# 2-Rhodaoxetanes: Their Formation of Oxidation of $[Rh^{I}(ethene)]^{+}$ and Their Reactivity upon Protonation

**Bas de Bruin, Mark J. Boerakker, Johanna A. W. Verhagen, René de Gelder, Jan M. M. Smits, and Anton W. Gal*[a]**

**Abstract:** New cationic, pentacoordinate complexes $[(TPA)Rh^{I}(ethene)]^{+}$, $[\mathbf{1a}]^{+}$, and $[(MeTPA)Rh^{I}(ethene)]^{+}$, $[\mathbf{1b}]^{+}$, have been prepared (TPA = *N*,*N*,*N*-tri(2-pyridylmethyl)amine, MeTPA = *N*-[(6-methyl-2-pyridyl)-methyl]-*N*,*N*-di(2-pyridylmethyl)amine). Complex $[\mathbf{1a}]^{+}$ is selectively converted by aqueous HCl to $[(TPA)Rh^{III}(ethyl)Cl]^{+}$, $[\mathbf{2a}]^{+}$. The same reaction with $[\mathbf{1b}]^{+}$ results in the $[(MeTPA)Rh^{III}(ethyl)Cl]^{+}$ isomers $[\mathbf{2b}]^{+}$ and $[\mathbf{2c}]^{+}$. Treatment of $[\mathbf{1a}]^{+}$ and $[\mathbf{1b}]^{+}$ with aqueous $H_2O_2$ results in a selective oxygenation to the unsubstituted 2-rhoda(III)oxetanes (1-oxa-2-rhoda(III)cyclobutanes) $[(TPA)Rh^{III}(\kappa^2\text{-}C,O\text{-}2\text{-}oxyethyl)]^{+}$, $[\mathbf{3a}]^{+}$, and $[(MeTPA)Rh^{III}(\kappa^2\text{-}C,O\text{-}2\text{-}oxyethyl)]^{+}$, $[\mathbf{3b}]^{+}$. The reactivity of 2-rhodaoxetanes $[\mathbf{3a}]^{+}$ and $[\mathbf{3b}]^{+}$ is dominated by the nucleophilic character of their 2-oxyethyl oxygen. Reaction of $[\mathbf{3a}]^{+}$ and $[\mathbf{3b}]^{+}$ with the non-coordinating acid $HBAr^{f}_{4}$ results in the dicationic protonated 2-rhodaoxetanes $[(TPA)Rh^{III}(\kappa^2\text{-}2\text{-}hydroxyethyl)]^{2+}$, $[\mathbf{4a}]^{2+}$, and $[(MeTPA)Rh^{III}(\kappa^2\text{-}2\text{-}hydroxyethyl)]^{2+}$, $[\mathbf{4b}]^{2+}$. These eliminate acetaldehyde at room temperature, probably via a coordinatively unsaturated $\kappa^1$-2-hydroxyethyl complex. In acetonitrile, complex $[\mathbf{4a}]^{2+}$ is stabilised as $[(TPA)Rh^{III}(\kappa^1\text{-}2\text{-}hydroxyethyl)(MeCN)]^{2+}$, $[\mathbf{5a}]^{2+}$, whereas the MeTPA analogue $[\mathbf{4b}]^{2+}$ continues to eliminate acetaldehyde. Reaction of $[\mathbf{3a}]^{+}$ with $NH_4Cl$ and MeI results in the coordinatively saturated complexes $[(TPA)Rh^{III}(\kappa^1\text{-}2\text{-}hydroxyethyl)(Cl)]^{+}$, $[\mathbf{6a}]^{+}$, and $[(TPA)Rh^{III}(\kappa^1\text{-}2\text{-}methoxyethyl)(I)]^{+}$, $[\mathbf{7a}]^{+}$, respectively. Reaction of $[\mathbf{3a}]^{+}$ with $NH_4^{+}$ in MeCN results in formation of the dicationic metallacyclic amide $[(TPA)Rh^{III}\{\kappa^2\text{-}O,C\text{-}2\text{-}(acetylamino)ethyl\}]^{2+}$, $[\mathbf{9}]^{2+}$, via the intermediates $[\mathbf{4a}]^{2+}$, $[\mathbf{5a}]^{2+}$ and the metallacyclic iminoester $[(TPA)Rh^{III}\{\kappa^2\text{-}N,C\text{-}2\text{-}(acetimidoyloxy)ethyl\}]^{2+}$, $[\mathbf{8}]^{2+}$. The observed overall conversion of the $[Rh^{I}(ethene)]$ complex $[\mathbf{1a}]^{+}$ to the metallacyclic amide $[\mathbf{9}]^{2+}$ via 2-rhodaoxetane $[\mathbf{3a}]^{+}$, provides a new route for the amidation of a $[Rh^{I}(ethene)]$ fragment.

**Keywords:** alkene complexes · amidations · metallaoxetanes · oxygenations · rhodium

## Introduction

2-Metallaoxetanes (1-oxa-2-metallacyclobutanes) have been proposed as intermediates in a number of synthetic conversions, such as the Mn-catalysed (asymmetric) epoxidation of olefins[1] and other epoxidation reactions,[2] stoichiometric and catalytic dihydroxylation of olefins by $KMnO_4$, $CrO_2Cl_2$ and $OsO_4$,[3] Rh-catalysed catalytic rearrangement of epoxides to ketones,[4] and Rh-catalysed asymmetric hydrogenolysis of epoxides.[5]

There have been no direct observations of 2-metallaoxetane intermediates in any of these reactions; mechanistic proposals have all been based on indirect evidence (e. g. kinetics). Reports on the reactivity of 2-metallaoxetanes are scarce and little is known about the properties of these strained four-membered metallacycles. The few isolated 2-metallaoxetanes are stabilised by various substituents.[6, 7] Consequently, it is difficult to deduce the intrinsic reactivity of the unsubstituted 2-metallaoxetane core of these examples. Previous results with phosphane-stabilised 2-rhodaoxetanes suggested that substituents at the $\beta$-position are required to prevent $\beta$-hydrogen elimination.[8]

We now describe the synthesis and reactivity of unsubstituted 2-rhoda(III)oxetanes obtained as isolable compounds by the selective oxygenation of nucleophilic cationic rhodium(I)-ethene complexes of the tetradentate N-ligands TPA (*N*,*N*,*N*-tri(2-pyridylmethyl)amine) and MeTPA (*N*-[(6-methyl-2-pyridyl)methyl]-*N*,*N*-di(2-pyridylmethyl)amine).

The reactivity of the obtained unsubstituted 2-rhodaoxetanes is mainly determined by the nucleophilic character of the 2-rhodaoxetane oxygen. Part of this work has already been communicated.[9]

[a] Prof. Dr. A. W. Gal, Dr. B. de Bruin, M. J. Boerakker, J. A. W. Verhagen, Dr. R. de Gelder, J. M. M. Smits
Department of Inorganic Chemistry, University of Nijmegen
Toernooiveld 1, NL-6525 ED Nijmegen (The Netherlands)
Fax: (+31) 24-355-3450
E-mail: gal@sci.kun.nl



0947-6539/00/0601-0298 $ 17.50+.50/0 *Chem. Eur. J.* **2000**, *6*, No. 1

## Results and Discussion

### Synthesis of the ethene complexes

We synthesised the ethene complexes $[(TPA)Rh^{I}(ethene)]^{+}$, $[\mathbf{1a}]^{+}$, and $[(MeTPA)Rh^{I}(ethene)]^{+}$, $[\mathbf{1b}]^{+}$, by the route shown in Scheme 1. $[\{(C_2H_4)_2Rh(\mu\text{-}Cl)\}_2]$ was stirred with TPA or MeTPA in MeOH at $-78\,^{\circ}C$ to afford [**1a**]Cl and [**1b**]Cl, respectively. Cations $[\mathbf{1a}]^{+}$ and $[\mathbf{1b}]^{+}$ were isolated as [**1a**]$BF_4$, [**1a**]$PF_6$ and [**1b**]$BPh_4$ by precipitation with $NaBF_4$, $KPF_6$ and $NaBPh_4$, respectively.

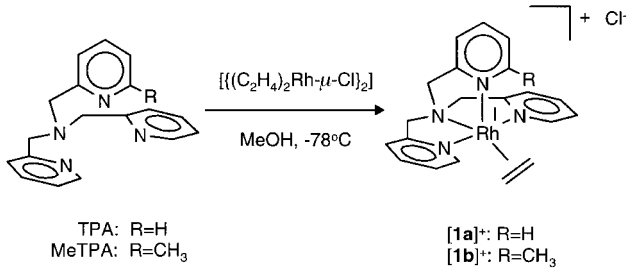


Scheme 1. Preparation of $Rh^{I}$(ethene) complexes $[\mathbf{1a}]^{+}$ and $[\mathbf{1b}]^{+}$.

The structure of [**1b**]$BPh_4$ was determined by single-crystal X-ray diffraction (Figure 1). Selected bond lengths and angles are given in Tables 1 and 2.

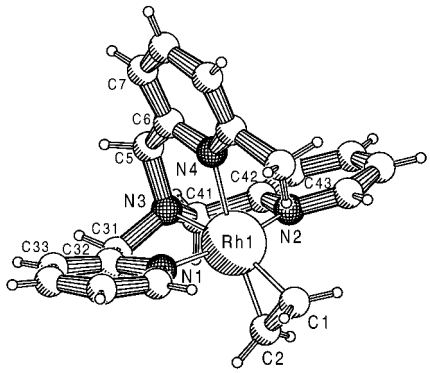


Figure 1. X-ray structure of ethene complex $[\mathbf{1b}]^{+}$.

The X-ray structure clearly reveals the pseudo trigonal-bipyramidal geometry of $[\mathbf{1b}]^{+}$. The equatorial positions are occupied by the 6-methylpyridyl nitrogen ($N_{Py\text{-}Me}$), the amine nitrogen ($N_{amine}$) and the ethene ligand; the axial positions by the two pyridyl nitrogens ($N_{Py}$).

The shortest Rh–N bond lengths are Rh1–N1 (2.019(7) Å) and Rh1–N2 (2.021(6) Å). The Rh–$N_{amine}$ bond length (Rh1–N3) is 2.175(6) Å. The longest Rh–N bond length is $N_{Py\text{-}Me}$, Rh1–N4: 2.257(7) Å; this probably reflects a weakening of the Rh–N interaction as a result of steric hindrance upon introduction of a methyl group at the 6 position of the 2-pyridyl.[10–12]

The theoretical and experimental results reported by Rossi and Hoffmann indicate that for $d^8$-metals in a trigonal bipyramid, the strongest σ-donor ligand prefers the axial position while the π ligands prefer parallel coordination in the equatorial plane.[13] The arrangement of the ligands in $[\mathbf{1b}]^{+}$ is in good agreement with these results.

The Rh–C bond lengths in $[\mathbf{1b}]^{+}$ are rather short (Rh–C1: 2.074(10) Å, Rh–C2: 2.086(9) Å) compared to those reported for other $[Rh^{I}(ethene)]$ complexes (range found in the Cambridge Structural Database, Rh–C: 2.084 – 2.226 Å).

The $^{1}H$ and $^{13}C$ NMR data of $[\mathbf{1a}]^{+}$ show one unique, and two equivalent pyridyl fragments. The two equivalent pyridyl fragments reflect an effective mirror plane through $N_{amine}$, the ethene fragment and the unique pyridyl fragment. The chemical shifts of the pyridyl fragments indicate that the structure of $[\mathbf{1a}]^{+}$ in solution is Ave-coordinate. The $^{1}H$ NMR Py-H6 signals are diagnostic: the Py-H6 signal for the unique pyridyl fragment ($\delta = 9.4$) has shifted 0.9 ppm downfield relative to the free ligand ($\delta = 8.5$) as a result of coordination to the cationic rhodium centre. The signal for the two equivalent pyridyl fragments ($\delta = 8.2$) has shifted 0.3 ppm upfield as a result of the anisotropic shielding effect of the coordinated ethene fragment. The diastereotopic protons of the two equivalent N-$CH_2$-Py groups give rise to an AB-type pattern. The methylene group connected to the unique pyridyl gives rise to a singlet. The NMR spectra of $[\mathbf{1b}]^{+}$ are similar to those of $[\mathbf{1a}]^{+}$ and show two equivalent axial pyridyl fragments and one equatorial 6-methylpyridyl fragment, which is in agreement with the X-ray structure.

Table 1. Selected bond lengths [Å] of the synthesised complexes.[a]

| | $[\mathbf{1b}]^{+}$ | $[\mathbf{2b^A}]^{+}$ | $[\mathbf{2b^B}]^{+}$ | $[\mathbf{2c}]^{+}$ | $[\mathbf{3b^A}]^{+}$ | $[\mathbf{3b^B}]^{+}$ | $[\mathbf{6a}]^{+}$ | $[\mathbf{8}]^{2+}$ | $[\mathbf{9}]^{2+}$ |
|---|---|---|---|---|---|---|---|---|---|
| N1–Rh1 | 2.019(7) | 2.00(2) | 1.97(3) | 2.041(3) | 2.045(10) | 2.033(9) | 2.034(7) | 2.025(10) | 2.034(4) |
| N2–Rh1 | 2.021(6) | 2.00(2) | 1.98(3) | 2.099(3) | 2.021(6) | 2.019(8) | 2.041(8) | 2.065(10) | 2.048(4) |
| N3–Rh1 | 2.175(6) | 2.00(2) | 2.103(19) | 2.050(3) | 2.140(8) | 2.124(8) | 2.091(7) | 2.137(10) | 2.142(3) |
| N4–Rh1 | 2.257(7) | 2.371(17) | 2.373(19) | 2.182(3) | 2.132(10) | 2.079(13) | 2.044(8) | 2.048(10) | 2.007(4) |
| N5–Rh1 | – | – | – | – | – | – | – | 2.055(12) | – |
| C1–Rh1 | 2.074(10) | 1.99(5) | 2.078(18) | 2.107(4) | 2.070(7) | 2.075(8) | 2.194(9) | 2.043(12) | 2.063(5) |
| C2–Rh1 | 2.086(9) | – | – | – | 2.564(7) | 2.542(10) | – | – | – |
| O1–Rh1 | – | – | – | – | 2.000(5) | 2.013(6) | – | – | 2.051(3) |
| Cl1–Rh1 | – | 2.365(6) | 2.362(6) | 2.3634(10) | – | – | 2.385(4) | – | – |
| C1–C2 | 1.445(16) | 1.51(5) | 1.52(3) | 1.486(6) | 1.514(11) | 1.49(2) | 1.62(3) | 1.473(17) | 1.496(9) |
| C2–O1 | – | – | – | – | 1.446(10) | 1.435(14) | 1.67(3) | 1.450(17) | – |
| C2–N5 | – | – | – | – | – | – | – | – | 1.443(7) |
| C3–O1 | – | – | – | – | – | – | – | 1.374(17) | 1.261(5) |
| C3–N5 | – | – | – | – | – | – | – | 1.245(19) | 1.319(6) |
| C3–C4 | – | – | – | – | – | – | – | 1.51(2) | 1.487(6) |

[a] For atom labelling see Figures 1, 2, 3, 5 and 6. Superscripts A and B distinguish independent cations in the unit cell.

  0947-6539/00/0601-0299 $ 17.50+.50/0 

Table 2. Selected bond angles and torsion angles [°] in the synthesised complexes.[a]

| | [**1b**]$^+$ | [**2b$^A$**]$^+$ | [**2b$^B$**]$^+$ | [**2c**]$^+$ | [**3b$^A$**]$^+$ | [**3b$^B$**]$^+$ | [**6a**]$^+$ | [**8**]$^{2+}$ | [**9**]$^{2+}$ |
|---|---|---|---|---|---|---|---|---|---|
| N1-Rh1-N2 | 164.5(2) | 164.8(7) | 163.5(9) | 163.61(12) | 163.5(3) | 165.6(3) | 164.3(3) | 164.4(4) | 164.1(1) |
| N1-Rh1-N3 | 81.3(2) | 84.6(7) | 82.1(7) | 83.21(11) | 80.6(4) | 81.3(4) | 82.6(3) | 82.1(5) | 82.2(1) |
| N1-Rh1-N4 | 93.0(2) | 81.1(8) | 79.6(8) | 84.60(12) | 98.4(4) | 94.0(5) | 87.7(3) | 91.2(4) | 91.4(1) |
| N1-Rh1-N5 | – | – | – | – | – | – | – | 90.7(5) | – |
| N2-Rh1-N3 | 83.3(2) | 81.0(7) | 81.4(9) | 80.54(12) | 83.6(3) | 84.4(4) | 81.9(3) | 82.4(5) | 82.4(1) |
| N2-Rh1-N4 | 84.4(2) | 101.5(8) | 99.3(8) | 95.18(12) | 83.7(4) | 85.4(4) | 92.8(3) | 88.2(4) | 90.9(2) |
| N2-Rh1-N5 | – | – | – | – | – | – | – | 88.3(5) | – |
| N3-Rh1-N4 | 76.8(3) | 82.0(8) | 81.4(8) | 82.23(11) | 81.1(4) | 81.8(4) | 82.9(3) | 82.3(4) | 82.8(1) |
| N3-Rh1-N5 | – | – | – | – | – | – | – | 92.0(5) | – |
| N4-Rh1-N5 | – | – | – | – | – | – | – | 173.6(5) | – |
| Rh1-C1-C2 | 70.1(5) | 116(2) | 113.4(17) | 115.2(3) | 90.0(5) | 89.4(6) | 103.5(12) | 115.0(9) | 111.7(4) |
| C1-C2-Rh1 | 69.2(6) | – | – | – | 53.8(4) | 54.7(4) | – | – | – |
| C1-Rh1-C2 | 40.6(5) | – | – | – | 36.2(3) | 35.9(4) | – | – | – |
| C1-C2-O1 | – | – | – | – | 104.6(6) | 106.4(7) | 102.3(19) | 116.0(13) | – |
| C1-C2-N5 | – | – | – | – | – | – | – | – | 114.5(5) |
| C2-O1-Rh1 | – | – | – | – | 94.8(4) | 93.5(6) | – | – | – |
| C1-Rh1-O1 | – | – | – | – | 70.3(3) | 70.0(4) | – | – | 91.1(2) |
| C2-Rh1-O1 | – | – | – | – | 34.2(3) | 34.3(4) | – | – | – |
| O1-C2-Rh1 | – | – | – | – | 51.0(3) | 52.2(4) | – | – | – |
| C2-O1-C3 | – | – | – | – | – | – | – | 118.1(13) | – |
| C2-N5-C3 | – | – | – | – | – | – | – | – | 124.9(5) |
| C3-N5-Rh1 | – | – | – | – | – | – | – | 129.8(13) | – |
| C3-O1-Rh1 | – | – | – | – | – | – | – | – | 126.8(3) |
| N5-Rh1-C1 | – | – | – | – | – | – | – | 87.8(5) | – |
| C1-Rh1-Cll | – | 87.8(8) | 83.8(6) | 85.76(11) | – | – | 93.9(3) | – | – |
| N5-C3-O1 | – | – | – | – | – | – | – | 126.3(18) | 121.4(5) |
| N5-C3-C4 | – | – | – | – | – | – | – | 125.7(16) | 119.7(5) |
| O1-C3-C4 | – | – | – | – | – | – | – | 108.0(17) | 118.9(4) |
| C1-Rh1-N1 | 97.1(3) | 91.6(10) | 94.0(9) | 89.03(14) | 96.4(4) | 96.3(4) | 97.3(3) | 96.2(5) | 97.1(2) |
| C1-Rh1-N2 | 96.9(3) | 84.4(10) | 86.4(9) | 90.69(14) | 98.1(3) | 97.3(4) | 98.4(3) | 99.4(5) | 98.3(2) |
| C1-Rh1-N3 | 158.3(4) | 92.3(10) | 96.2(8) | 96.22(13) | 167.7(3) | 166.6(4) | 175.7(3) | 178.2(5) | 179.0(2) |
| C1-Rh1-N4 | 124.8(4) | 171.1(9) | 173.4(8) | 173.58(13) | 111.2(4) | 111.6(5) | 92.8(3) | 98.0(5) | 96.4(2) |
| C1-Rh1-N5 | – | – | – | – | – | – | – | 87.8(5) | – |
| O1-Rh1-N1 | – | – | – | – | 85.9(3) | 90.6(3) | – | – | 88.8(1) |
| O1-Rh1-N2 | – | – | – | – | 91.5(3) | 89.6(3) | – | – | 86.9(1) |
| O1-Rh1-N3 | – | – | – | – | 97.6(3) | 96.8(3) | – | – | 89.6(1) |
| O1-Rh1-N4 | – | – | – | – | 175.2(4) | 174.9(4) | – | – | 172.4(1) |
| Cl1-Rh1-N1 | – | 97.2(5) | 97.1(5) | 91.66(9) | – | – | 91.7(3) | – | – |
| Cl1-Rh1-N2 | – | 97.2(6) | 99.4(8) | 104.66(9) | – | – | 86.0(2) | – | – |
| Cl1-Rh1-N3 | – | 178.2(6) | 179.2(6) | 174.45(8) | – | – | 90.4(2) | – | – |
| Cl1-Rh1-N4 | – | 98.0(5) | 98.6(6) | 95.23(8) | – | – | 173.27(19) | – | – |
| C2-Rh1-N1 | 92.5(3) | – | – | – | – | – | – | – | – |
| C2-Rh1-N2 | 93.8(3) | – | – | – | – | – | – | – | – |
| C2-Rh1-N3 | 117.7(4) | – | – | – | – | – | – | – | – |
| C2-Rh1-N4 | 165.1(4) | – | – | – | – | – | – | – | – |
| Rh1-N3-C31-C32 | – 44.0(6) | 36(2) | – 38(3) | – 34.5(4) | – 42.0(8) | – 43.1(9) | – 39.2(8) | 39.8(13) | – 38.3(4) |
| Rh1-N3-C41-C42 | 42.5(6) | – 35.8(19) | 31(4) | 41.4(3) | 36.2(9) | 37.8(8) | 37.6(8) | – 35.1(13) | 33.7(6) |
| Rh1-N3-C5-C6 | – 13.0(8) | – 33(3) | 40(3) | 27.3(4) | – 27.1(9) | – 19.5(12) | 12.1(8) | 7.0(14) | – 5.4(5) |
| N3-C31-C32-N1 | 37.5(8) | – 28(3) | 30(3) | 30.4(5) | 31.5(12) | 34.8(12) | 32.7(11) | – 32.1(17) | 27.7(6) |
| N3-C41-C42-N2 | – 40.9(8) | 22(2) | – 21(5) | – 25.7(5) | – 36.0(12) | – 32.1(10) | – 27.6(12) | 30.0(18) | – 25.3(7) |
| N3-C5-C6-N4 | 16.2(9) | 49(3) | – 58(4) | – 33.8(4) | 33.2(13) | 27.2(16) | – 16.0(11) | – 5.2(19) | 5.6(7) |

[a] For atom labelling see Figures 1, 2, 3, 5 and 6. Superscripts $^A$ and $^B$ distinguish independent cations in the unit cell.

Intramolecular exchange of donor atoms is known to proceed very rapidly in five-coordinate $Rh^I$ complexes. Therefore, it is remarkable that the axial and equatorial pyridyl groups in [**1a**]$^+$ do not exchange on the NMR time scale at room temperature. In both the $^1H$ and $^{13}C$ NMR spectra of [**1a**]$^+$ at 298 K, the ethene fragment is observed as two broad signals. At 263 K the ethene rotation is frozen out, and the two inequivalent $=CH_2$ fragments are observed as two pseudo double-triplets in the $^1H$ NMR spectrum and two doublets in the $^{13}C$ NMR spectrum.

**Reactivity of the ethene complexes**

We studied the reactivity of the ethene complexes towards aqueous HCl and aqueous $H_2O_2$. Protonation of [**1a**]$^+$ by HCl results in the formation of [(TPA)$Rh^{III}$(ethyl)(Cl)]$^+$, [**2a**]$^+$. The analogous reaction of [**1b**]$^+$ yields isomer [**2b**]$^+$ or [**2c**]$^+$, depending on the reaction conditions. Oxidation of [**1a**]$^+$ and [**1b**]$^+$ with aqueous $H_2O_2$ results in the selective formation of 2-rhoda(III)oxetanes [**3a**]$^+$ and [**3b**]$^+$, respectively (Scheme 2).



0947-6539/00/0601-0300 $ 17.50+.50/0 *Chem. Eur. J.* **2000**, *6*, No. 1

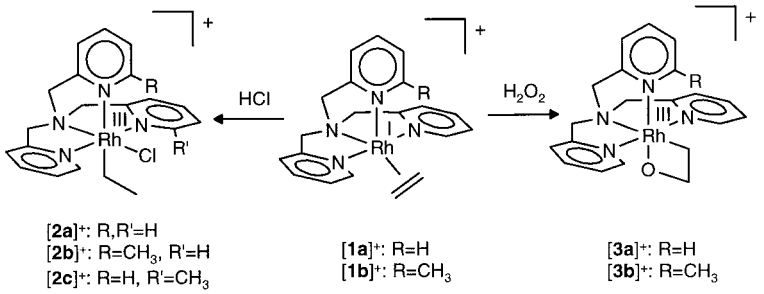


Scheme 2. Reaction of $[\mathbf{1a}]^+$ and $[\mathbf{1b}]^+$ with aqueous HCl and aqueous $H_2O_2$.

**Protonation to ethyl complexes**: The reaction of the ethene complex [**1a**]Cl (prepared in situ) with HCl in MeOH results in the formation of [(TPA)$Rh^{III}$(ethyl)(Cl)]Cl, [**2a**]Cl. Compound $[\mathbf{2a}]^+$ was precipitated as its $PF_6^-$ salt by the addition of $KPF_6$. The reaction of [**1b**]Cl with HCl results in two isomeric ethyl-chloro complexes; either the symmetric [**2b**]Cl, or the asymmetric [**2c**]Cl is formed, depending on the reaction conditions. Symmetric [**2b**]Cl was obtained by the addition of a high concentration of HCl to a solution of [**1b**]Cl at $-78\,^\circ C$ followed by slow warming to room temperature; the asymmetric isomer [**2c**]Cl was obtained by the addition of a lower concentration of HCl to a solution of [**1b**]Cl at $-78\,^\circ C$ followed by a faster warming to room temperature. The $BPh_4^-$ salts [**2b**]$BPh_4$ and [**2c**]$BPh_4$ were isolated by precipitation with $NaBPh_4$. (Scheme 2).

The above results clearly demonstrate the nucleophilic character of the cationic [$Rh^I$(ethene)] species $[\mathbf{1a}]^+$ and $[\mathbf{1b}]^+$. Although protonation of neutral [$Rh^I$(ethene)] and [$Ir^I$(ethene)] complexes to give the $M^{III}$–ethyl species has been reported previously,[14] the protonation of cationic [$Rh^I$(ethene)] complexes is unprecedented. As shown by $^1H$ NMR, the ethene fragment in [**1a**]$BF_4$ is also protonated upon treatment with $HBF_4 \cdot (OEt_2)_2$ in $CH_2Cl_2$. This indicates that the protonation does not require a coordinating anion or a coordinating solvent.

The structures of isomers [**2b**]$BPh_4$ and [**2c**]$BPh_4$ were determined by single-crystal X-ray diffraction (Figure 2 and Figure 3). For $[\mathbf{2b}]^+$, two independent cations, $[\mathbf{2b^A}]^+$ and $[\mathbf{2b^B}]^+$, are found per unit cell. Selected bond lengths and angles are given in Tables 1 and 2.

The X-ray structures of isomers $[\mathbf{2b}]^+$ and $[\mathbf{2c}]^+$ show that both are pseudo-octahedral and confirm that the observed isomerism results from the exchange of positions by Py and $Py^{Me}$ and *not* by chloride and ethyl. In the X-ray structure of $[\mathbf{2c}]^+$, the longest Rh–$N_{Py}$ bond length is observed for the $N_{py}$ which lies *trans* to the ethyl group (Rh1–N4: 2.182(3) Å). This reflects the high *trans* influence of the ethyl fragment. In the lower quality X-ray structure of $[\mathbf{2b}]^+$, the corresponding Rh–$N_{py\text{-}Me}$ bond length *trans* to ethyl seems to be even longer($[\mathbf{2b^A}]^+$: Rh1–N4: 2.371(17) Å; $[\mathbf{2b^B}]^+$: Rh1–N4: 2.373(19) Å). The elongation of the Rh–N4 bond and the increased puckering of the -Rh1-N3-C5-C6-N4- chelate ring from $[\mathbf{2c}]^+$ to $[\mathbf{2b}]^+$,(as a result of torsion around the N3–C5 and C5–C6 bonds, see Table 2) seem to reflect an increased steric hinderance of the Rh–N4 interaction upon substitution of $N_{Py}$ by $N_{Py\text{-}Me}$ (vide supra).[10–12] Rh–N bond lengths of N-donors *trans* to ethyl in (N ligand)–$Rh^{III}$–ethyl complexes, had so far been observed in the range 2.207–2.256 Å.[15] The $^1H$ NMR spectra of $[\mathbf{2a}]^+$ and $[\mathbf{2b}]^+$ (Scheme 2) show one unique and two equivalent pyridyl fragments, in accordance with the X-ray structure of $[\mathbf{2b}]^+$. The NMR data for the ethyl fragments of $[\mathbf{2a}]^+$, $[\mathbf{2b}]^+$ and $[\mathbf{2c}]^+$ are given in Tables 3 and 4. In the $^1H$ NOESY spectrum of $[\mathbf{2a}]^+$, a clear NOE contact is observed between the methylene protons of the ethyl fragment and the nearby axial methylene protons (one of the two AB-type doublets) of the two equivalent N-$CH_2$-Py fragments, in accordance with a *trans* orientation of the ethyl group and the unique pyridyl

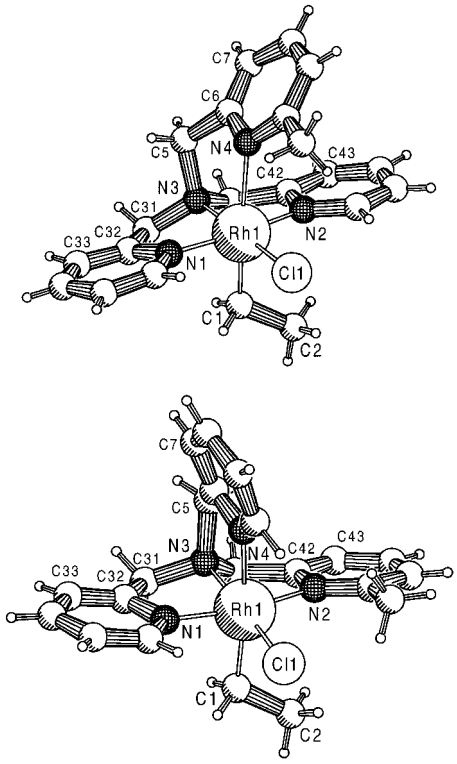


Figure 2. X-ray structures of symmetric ethyl–chloro complex $[\mathbf{2b^A}]^+$ (top) and asymmetric ethyl-chloro complex $[\mathbf{2c}]^+$ (bottom).

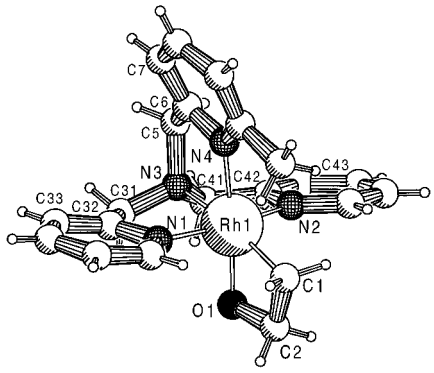


Figure 3. X-ray structure of 2-rhoda(III)oxetane $[\mathbf{3b}]^+$.

fragment. The $^1$H NMR spectrum of asymmetric isomer [**2c**]$^+$ shows three AB-type signals for the three N-$CH_2$-Py methylene groups, in accordance with the X-ray structure (Figure 2). The protons of the Rh–ethyl fragment give rise to a triplet at $\delta = 0.56$ and two multiplets at $\delta = 2.56$ and $\delta = 2.79$, for the methyl fragment and the two diastereotopic methylene protons, respectively (Table 3).

Table 3. $^1$H NMR chemical shifts and coupling constants of the Rh-$CH_2$-$CH_2$-Y fragments.

| | Solvent | Y | $\delta$(Rh-$CH_2$-) | $\delta$(-$CH_2$-Y-) | $^3J$(H,H) (±0.2 Hz) | $^2J$(Rh,H) (±0.2 Hz) |
|---|---|---|---|---|---|---|
| [**2a**]$^+$ | [D$_6$]acetone | H | 2.71 | 0.61 | 7.4 | 2.7 |
| [**2b**]$^+$ | $CD_2Cl_2$ | H | 2.71 | 0.36 | 7.4 | 2.7 |
| [**2c**]$^+$ | $CD_2Cl_2$ | H | 2.79, 2.56 | 0.56 | 7.4 | unclear |
| [**3a**]$^+$ | $CD_2Cl_2$ | O | 2.25 | 4.98 | 7.5 | 2.4 |
| | [D$_6$]acetone | | 2.35 | 4.97 | 7.5 | 2.5 |
| [**3b**]$^+$ | $CD_2Cl_2$ | O | 2.35 | 4.80 | 7.6 | 2.6 |
| | [D$_6$]acetone | | 2.45 | 4.87 | 7.5 | 2.6 |
| [**4a**]$^{2+}$ | $CD_3CN$ | O | 2.95 | 5.38 | 8.1 | 2.1 |
| [**4b**]$^{2+}$ | $CD_2Cl_2$ | O | 3.09 | 5.16 | 8.1 | 2.1 |
| | $CD_3CN$ | | 3.12 | 5.21 | 8.1 | 2.4 |
| [**5a**-D$_3$]$^{2+}$ | $CD_3CN$ | O | 3.23 | 4.01 | 7.5 | 2.6 |
| [**6a**]$^+$ | $CD_2Cl_2$ | O | 3.18 | 3.96 | 5.3 | 2.6 |
| | [D$_6$]acetone | | 3.35 | 4.03 | 6.2 | 2.6 |
| | $CD_3CN$ | | 3.16 | 3.98 | 7.9 | 2.6 |
| | [D$_6$]DMSO | | 3.13 | 3.96 | 8.2 | 2.6 |
| [**7a**]$^+$ | $CD_2Cl_2$ | O | 3.28 | 4.08 | 6.3 | 2.9 |
| [**8**]$^{2+}$ | $CD_3CN$ | O | 3.38 | 4.26 | 5.6 | 2.7 |
| [**9**]$^{2+}$ | $CD_3CN$ | N | 3.47 | 3.23 | 5.9 | 2.4 |
| [**10**]$^+$ | [D$_6$]acetone | O | 3.16 | 3.57 | 5.6 | 2.7 |

A feasible mechanism for formation of the $Rh^{III}$–ethyl–chloro complexes would be the formation of a [$Rh^{III}$(ethyl)] fragment by direct protonation at the ethene fragment,[16] in accordance with significant rhoda(III)-cyclopropane character of the $Rh^I$(ethene) fragment. An alternative mechanism would be the protonation of the $Rh^I$ centre to give a $Rh^{III}$-hydride species. Subsequent migratory insertion of ethene into the Rh–H bond would then result in the formation of [**2a**]$^+$, [**2b**]$^+$ and [**2c**]$^+$. Precedents for the protonation of $Rh^I$ and $Ir^I$ sites to $Rh^{III}$–H and $Ir^{III}$–H sites (some in equilibrium with $M^{III}$–ethyl species) are known.[17] The two isomers [**2b**]$^+$ and [**2c**]$^+$ could result from the protonation of a symmetric and an asymmetric isomer of the ethene complex [**1b**]$^+$.

**Oxygenation to 2-rhodaoxetanes**: The reaction of ethene complex [**1a**]$PF_6$ with an excess of aqueous $H_2O_2$ (35%) in MeOH at $-10\,^\circ$C resulted in the immediate selective oxygenation to 2-rhodaoxetane [**3a**]$PF_6$ (Scheme 2). The $BPh_4^-$ salt [**3a**]$BPh_4$ was obtained by in situ oxidation of [**1a**]Cl (vide supra) with $H_2O_2$ and precipitation by the addition of $NaBPh_4$ (1 equiv). Similarly, we obtained [**3b**]$BPh_4$ by in situ oxygenation of [**1b**]Cl. The reactions result in a colour change of the solution from yellow to pale yellow.

Clear signals for the Rh-$CH_2$-$CH_2$-O- fragments are observed in the $^1$H and $^{13}$C NMR spectra of [**3a**]$^+$ and [**3b**]$^+$ (Tables 3 and 4).

In the $^1$H NMR spectra, the -$CH_2$-O- protons are observed as triplets whereas the Rh-$CH_2$- protons are observed as doublets of triplets as a result of rhodium coupling. The -Rh-$CH_2$- signals in $^1$H NMR and $^{13}$C NMR appear significantly upfield compared to those for the ethyl compounds [**2a**]–[**2c**]$^+$. In the $^{13}$C NMR spectra, both the -$CH_2$-O- and the Rh-$CH_2$- signals show rhodium coupling. The $^1J(^{103}Rh,^{13}C)$ coupling of -Rh-$CH_2$- in [**3a**]$^+$ and [**3b**]$^+$ is significantly smaller than those in all other compounds in Table 4, which is possibly related to the ring strain in [**3a**]$^+$ and [**3b**]$^+$. The $^2J(^{103}Rh,^{13}C)$ coupling of the -$CH_2$-O- fragment in [**3a**]$^+$ and [**3b**]$^+$ is lost upon dissociation of the Rh–O bond (vide infra).

Table 4. $^{13}$C NMR chemical shifts and coupling constants of the Rh-$CH_2$-$CH_2$-Y fragments.

| | Solvent | Y | $\delta$(Rh-$CH_2$-) | $\delta$(-$CH_2$-Y-) | $^1J$(C,Rh) [±0.2 Hz] | $^2J$(C,Rh) [±0.2 Hz] |
|---|---|---|---|---|---|---|
| [**2a**]$^+$ | [D$_6$]acetone | H | 15.4 | 16.9 | 21.9 | 0 |
| [**2b**]$^+$ | $CD_2Cl_2$ | H | 20.9 | 17.8 | 23.6 | 0 |
| [**2c**]$^+$ | $CD_2Cl_2$ | H | 17.5 | 17.8 | 20.4 | 0 |
| [**3a**]$^+$ | [D$_6$]acetone | O | 1.3 | 78.7 | 18.4 | 4.0 |
| [**3b**]$^+$ | [D$_6$]acetone | O | 2.5 | 80.6 | 18.0 | 4.2 |
| [**6a**]$^+$ | [D$_6$]DMSO | O | 34.4 | 64.6 | 25.0 | 0 |
| [**7a**]$^+$ | $CD_2Cl_2$ | O | 26.3 | 79.8 | 25.0 | 0 |
| [**8**]$^{2+}$ | [D$_6$]DMSO | O | 28.4 | 71.8 | 26.6 | 0 |
| [**9**]$^{2+}$ | [D$_6$]DMSO | N | 33.3 | 41.5 | 27.7 | 0 |

To the best of our knowledge, [**3a**]$^+$ and [**3b**]$^+$ are the first isolated examples of unsubstituted 2-metallaoxetanes. Substituted[6] 2-metallaoxetanes have been prepared by oxidative addition of epoxides to $Rh^I$, $Pt^0$ and Pd complexes,[7a, 7b, 8b] or, in the case of 2-rhoda- and 2-iridaoxetanes, by the deprotonation of a $\beta$-hydroxyethyl-metal-halide complex,[7c, 8] and by oxygenation of the cycloctadiene (cod) complex [$(P_3O_9)Ir^I$(cod)]$^{2-}$ with dioxygen.[7d] The observed oxygenation of [**1a**]$^+$ and [**1b**]$^+$ to [**3a**]$^+$ and [**3b**]$^+$ are the first examples of the oxidation of an ethene complex to a 2-metallaoxetane.

The crystal structure of [**3b**]$BPh_4 \cdot 1.5\,H_2O$ was determined by single-crystal X-ray diffraction. The unit cell proved to contain a pseudo-centrosymmetric arrangement of two cations ([**3b$^A$**]$^+$ and [**3b$^B$**]$^+$), two anions as well as three water molecules. The molecular structure of cation [**3b$^A$**]$^+$ is shown in Figure 3.

Two-thirds of the water molecules in crystalline [**3b**]$BPh_4 \cdot 1.5\,H_2O$ are found as independent water dimers. Interestingly, one-third of the water molecules connect the cations [**3b$^A$**]$^+$ and [**3b$^B$**]$^+$ through two $O_{water}$–H$\cdots O_{oxetane}$ hydrogen bonds (Figure 4). The $O_{water}$ atoms are also involved in a bifurcated

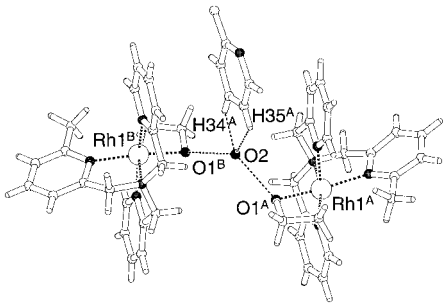


Figure 4. Crystal structure of [**3b**]$BPh_4 \cdot 1.5\,H_2O$ including the hydrogen-bridging water molecule.



0947-6539/00/0601-0302 $ 17.50+.50/0 *Chem. Eur. J.* **2000**, *6*, No. 1

hydrogen bond with pyridyl-H34$^A$ and -H35$^A$ of a neighbouring $[\mathbf{3b^A}]^+$ ion. Interatomic distances: O2–O1$^A$ 2.645(6) Å, O2–O1$^B$ 2.713(7) Å, O2–H34$^A$ 1.900(15) Å, O2–H35$^A$ 2.037(11) Å (Figure 4). The observed hydrogen bonding of $H_2O$ to the 2-rhodaoxetane fragment parallels the frequently observed hydrogen bonding between alcohols and late transition-metal alkoxides.[18] The water signal from $[\mathbf{3b}]BPh_4 \cdot 1.5\,H_2O$ in $CD_2Cl_2$ appears at $\delta = 2.05$ in the $^1$H NMR spectrum, which indicates that there is hydrogen bonding of water to the 2-rhodaoxetane oxygen in solution (free water in $CD_2Cl_2$: $\delta = 1.50$).

Rhodium-alkoxy compounds are rare. The Rh–O bond lengths in 2-rhodaoxetane $[\mathbf{3b}]^+$ are short ($[\mathbf{3b^A}]^+$: 2.000(5) Å, $[\mathbf{3b^B}]^+$: 2.013(6) Å) compared to the range of previously reported Rh–$O_{alkoxy}$ bond lengths (2.01–2.11 Å),[18a, 19] This range includes the Rh–$O_{alkoxy}$ bond length (2.10 Å) in the $\beta,\beta$-disubstituted 2-rhodaoxetane $[(PMe_3)_3(Br)Rh(\kappa^2\text{-}C,O\text{-}H_2C(Me)_2O)]$, **I**, the only isolated 2-rhodaoxetane reported to date.[8] The difference between the cationic $[\mathbf{3b}]^+$ and the neutral **I** could be the result of a weaker *trans* influence of the hard N donor in $[\mathbf{3b}]^+$ compared to the soft P donor in **I**. A M–O bond length of 1.96 Å, similar to that in $[\mathbf{3b}]^+$, is observed for the dianionic 2-iridaoxetane $[(P_3O_9)Ir(\text{'Ocod'})]^{2-}$, **II**.[7d] The C–O bond length for $[\mathbf{3b}]^+$ ($[\mathbf{3b^A}]^+$: 1.45 Å, $[\mathbf{3b^B}]^+$: 1.44 Å) is much shorter than the very long C–O bond length in the strained 2-iridaoxetane **II** (1.86 Å); however, it compares well with that in the 2-rhodaoxetane **I** (1.42 Å). The Rh–C and C–C bond lengths in 2-rhodaoxetane $[\mathbf{3b}]^+$ compare well with the corresponding bond lengths in **I** and **II**.[7d, 8] The longest Rh–N bond length is observed for the central amine, which reflects the high *trans* influence of the alkyl group (Rh1–N3 2.140(8), 2.124(8) Å).

As regards the mechanism of 2-rhodaoxetane formation: the reactions of the ethene complexes $[\mathbf{1a}]^+$ and $[\mathbf{1b}]^+$ with HCl, clearly demonstrate their nucleophilicity. One could therefore imagine electrophilic attack of $H_2O_2$ at the Rh$^I$ centre, which results in a net transfer of OH$^+$ to the Rh$^I$ centre.[20] Insertion of the ethene fragment into the so-obtained Rh$^{III}$–OH bond, followed by proton abstraction from the resulting 2-hydroxyethyl fragment would result in the 2-rhodaoxetane fragment. In view of the substantial rhoda(III)cyclopropane character of the rhodium-ethene fragment, 2-rhodaoxetane formation could also be the result of direct oxygenation of one of the ethene carbons. In this formalism, the oxidation of $[\mathbf{1a}]^+$ and $[\mathbf{1b}]^+$ to the 2-rhodaoxetanes bears some resemblance to the oxidation of a nickela(II)cyclopentane complex with $N_2O$ to a 1-oxa-2-nickela(II)cyclohexane.[21]

**Reactivity of the 2-rhodaoxetanes**

At room temperature the 2-rhodaoxetanes $[\mathbf{3a}]^+$ and $[\mathbf{3b}]^+$ are stable in solution and do not react with CO, $PPh_3$, ethene or acetylenes.

The 2-rhodaoxetane fragment is also stable toward strong bases. Treatment of a solution of $[\mathbf{3b}]^+$ in $CD_2Cl_2$ with a solution of $NaOCD_3$ in $CD_3OD$ has little effect on the $^1$H NMR signals of the 2-rhodaoxetane fragment; however, the signals of the methylene groups of the MeTPA ligand disappear from the $^1$H NMR spectrum. This indicates that $NaOCD_3$ catalysed the H/D exchange at N-$CH_2$-Py.

In the presence of acids, the reactivity of the 2-rhodaoxetane fragment is clearly increased, as is described below.

**Protonation and methylation of the 2-rhodaoxetane oxygen**: The hydrogen bonding of the 2-rhodaoxetane oxygen with water as shown by the X-ray structure of $[\mathbf{3b}]BPh_4$, provides a first indication of its strongly nucleophilic character. In accordance with this, treatment of the 2-rhodaoxetanes $[\mathbf{3a}]BPh_4$ and $[\mathbf{3b}]BPh_4$ with one equivalent of the non-coordinating acid $[H(OEt_2)_2]B(C_6H_3(CF_3)_2)_4$ $HBAr^f{}_4$,[22] in $CD_2Cl_2$ or $CD_3CN$, results in the protonated rhodaoxetanes $[\mathbf{4a}]BPh_4/BAr^f{}_4$ and $[\mathbf{4b}]BPh_4/BAr^f{}_4$ (Scheme 3).

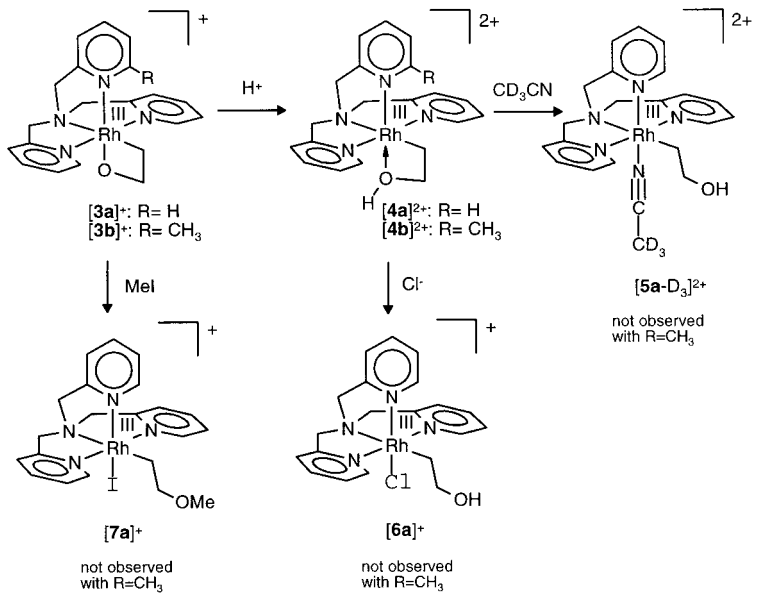


Scheme 3. Reaction of 2-rhoda(III)oxetanes $[\mathbf{3a}]^+$ and $[\mathbf{3b}]^+$ with electrophiles H$^+$, $NH_4Cl$, MeI and H$^+$/$CH_3CN$.

As observed by $^1$H NMR spectroscopy in $CD_2Cl_2$, $[\mathbf{4a}]^{2+}$ and $[\mathbf{4b}]^{2+}$ readily eliminate acetaldehyde at room temperature, whereas $[\mathbf{3a}]^{2+}$ and $[\mathbf{3b}]^{2+}$ are stable. In [D$_6$]DMSO, $[\mathbf{3a}]^+$ and $[\mathbf{3b}]^+$ only start to eliminate acetaldehyde at 90 °C. In $[\mathbf{4b}]^{2+}$, the elimination of acetaldehyde is also observed in $CD_3CN$ at room temperature. However, for $[\mathbf{4a}]^{2+}$ in $CD_3CN$, the elimination of acetaldehyde is blocked and quantitative conversion to $[(TPA)Rh^{III}(\kappa^1\text{-}C\text{-}2\text{-hydroxyethyl})(CD_3CN)]^{2+}$, $[\mathbf{5a}\text{-}D_3]^{2+}$ occurs within 1 h (Scheme 3). Complex $[\mathbf{5a}\text{-}D_3]^{2+}$ was only characterised by $^1$H NMR spectroscopy (Table 3) and FAB-MS. Attempts to isolate $[\mathbf{4a}]^{2+}$, $[\mathbf{4b}]^{2+}$ and $[\mathbf{5a}]^{2+}$ were unsuccessful because of their instability.

Protonation of [**3a**]$^+$ and [**3b**]$^+$ to the metallacyclic $\kappa^2$-*O*,*C*-2-hydroxyethyl complexes [**4a**]$^{2+}$ and [**4b**]$^{2+}$ results in a downfield shift 0.7 ppm for -Rh-$CH_2$- in the $^1$H NMR spectrum. Protonation to the non-cyclic $\kappa^1$-*C*-2-hydroxyethyl complex [**5a**-$D_3$]$^{2+}$ results in an even larger downfield shift of 1.0 ppm. These shifts could well reflect the release of ring strain. In [**4a**]$^+$ and [**4b**]$^+$, -$CH_2$-O- has shifted 0.4 ppm downfield from [**3a**]$^+$ and [**3b**]$^+$. In contrast, the open chain -$CH_2$-O- fragment in [**5a**-$D_3$]$^{2+}$ has shifted by 1.0 ppm upfield to a normal value for an alcohol (Table 3).

As mentioned above, protonation of the 2-rhodaoxetane oxygen results in the elimination of acetaldehyde at room temperature. This elimination must also involve $\beta$-hydrogen elimination. It seems reasonable to propose ring-opening of a protonated 2-rhodaoxetane to a Rh$^{III}$-$\kappa^1$-*C*-2-hydroxyethyl fragment with a vacant *cis* position, followed by a $\beta$-hydride shift and deprotonation to a formylmethyl hydride complex and reductive elimination of acetaldehyde (Scheme 4).

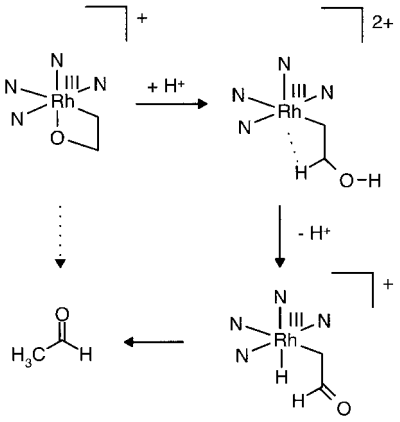


Scheme 4. Proposed mechanism for $\beta$-hydrogen elimination from protonated 2-rhoda(III)oxetanes.

The observed elimination of acetaldehyde at elevated temperatures in the absence of added acid (vide supra) might involve protonation of the 2-rhodaoxetane by traces of acid, but could also occur directly from the unprotonated 2-rhodaoxetane (Scheme 4). A formylmethyl hydride intermediate has also been proposed for the rhodium(I)-catalysed isomerisation of epoxides, via 2-rhodaoxetanes.[23] In agreement with this mechanism, a *cis*-hydrido-formylmethyl iridium(III) complex was obtained by the reaction of ethylene oxide with [$Ir^I(C_8H_{14})(PMe_3)_3(Cl)$].[24] For rhoda(III)- and irida(III)oxetanes, $\beta$-hydrogen elimination is apparently favoured over reductive elimination of an epoxide. In fact, reductive elimination of an epoxide from an isolated 2-metallaoxetane has never been reported.

Treatment of a solution of [**3a**]$BPh_4$ with $NH_4Cl$ in acetone resulted in the formation of [(TPA)Rh$^{III}$($\kappa^1$-*C*-2-hydroxyethyl)(Cl)]$BPh_4$ ([**6a**]$BPh_4$), presumably from the dissociation of the hydroxyethyl oxygen from the Rh$^{III}$ centre in intermediate [**4a**]$^{2+}$ and coordination of the chloride anion (Scheme 3).

Bright yellow crystals of [**6a**]$BPh_4\cdot$MeOH, which were suitable for X-ray diffraction, were obtained by slow crystallisation of [**6a**]$BPh_4$ from a solution in acetone that was layered with MeOH. The X-ray structure of [**6a**]$^+$ is shown in Figure 5. Selected bond lengths and angles are given in Tables 1 and 2.

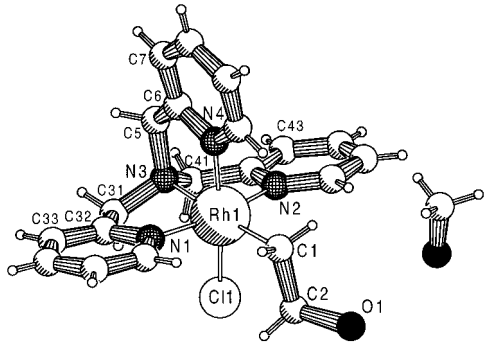


Figure 5. X-ray structure of 2-hydroxyethyl–chloro complex [**6a**]$^+\cdot$MeOH.

The quality of the X-ray structure suffers from of severe disorder in the $CH_2$-$CH_2$-OH fragment and the co-crystallised MeOH. This disorder could not be interpreted in terms of a physically reasonable disorder model. The X-ray diffraction data do, however, confirm the presence of the $\kappa^1$-*C*-2-hydroxyethyl fragment. The co-crystallised MeOH molecule seems to be involved in O–H$\cdots$O hydrogen bonding with the hydroxy fragment of [**6a**]$^+$. The structure of the 2-hydroxyethyl complex [**6a**]$^+$ is similar to those of the ethyl complexes [**2b**]$^+$ and [**2c**]$^+$. However, the 2-hydroxyethyl fragment of [**6a**]$^+$ is oriented *trans* to $N_{amine}$, whereas the ethyl fragments of [**2b**]$^+$ and [**2c**]$^+$ are oriented *trans* to $N_{Py\text{-}Me}$ and $N_{Py}$, respectively.

The chemical shifts of the Rh-$CH_2$- fragment and the -$CH_2$-O- fragment in the $^1$H and $^{13}$C NMR spectra of [**6a**]$^+$ are characteristic for a $\kappa^1$-*C*-2-hydroxyethyl fragment (see Tables 3 and 4). The coupling constant $^3J$(H,H) of [**6a**]$^+$ strongly increases on going from $CD_2Cl_2$ (5.3 Hz), the least polar solvent, to [$D_6$]DMSO (8.2 Hz), the most polar solvent (Table 3). We explain this solvent-dependent behaviour by assuming the presence of an equilibrium between an open form, as in the X-ray structure (Figure 5), and a cyclic form in which the 2-hydroxyethyl ligand of [**6a**]$^+$ donates an intramolecular hydrogen bond to the chloro ligand. In an apolar solvent the cyclic structure dominates, whereas in a polar solvent interactions with solvent molecules stabilise the open structure (Scheme 5). Strong intramolecular OH$\cdots$Cl hydrogen bonding between chloride and the OH group of a

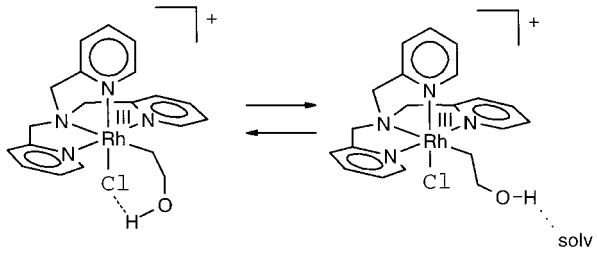


Scheme 5. Equilibrium between hydrogen-bonded cyclic and open structures of [**6a**]$^+$.



0947-6539/00/0601-0304 $ 17.50+.50/0 *Chem. Eur. J.* **2000**, *6*, No. 1

2-hydroxy-2,2-(dimethyl)ethyl fragment has been observed in the X-ray structure of [(Rh($PMe_3$)$_3$(Br)(Cl){$CH_2$C-(Me)$_2$OH}].[8] Hydrogen bonding has also been reported for other metal-bound halide ligands.[25]

The reaction of [**3a**]$BPh_4$ with MeI is analogous to the reaction with $NH_4Cl$: it results in the formation of [(TPA)-$Rh^{III}$(2-methoxyethyl)(I)]$BPh_4$ ([**7a**]$BPh_4$) (Scheme 3). Compound [**7a**]$BPh_4$ was isolated as bright-orange crystals from a saturated solution in $CH_3CN$. Nucleophilic attack by the oxygen atom of [**3a**]$^+$ on MeI releases iodide, which subsequently displaces the methylated oxygen from the $Rh^{III}$ centre. NMR data for the Rh-$CH_2$-$CH_2$-O fragment of [**7a**]$^+$ are summarised in Tables 3 and 4.

Attempts to prepare the MeTPA analogues of [**5a**]$^{2+}$, [**6a**]$^+$ and [**7a**]$^+$ from the MeTPA complex [**3b**]$^+$ resulted in complex reaction mixtures. The observed differences between [**3a**]$^+$ and [**3b**]$^+$ probably result from steric hindrance by the Py-Me fragment in [**3b**]$^+$. The Py-Me group hinders the rotation of the -$CH_2$-$CH_2$-OR (R = H, Me) fragments around the Rh–C bond. Dissociation of the Rh–O bond without rotation around Rh–C will hold the $\beta$-hydrogens close to the rhodium centre and thus promote $\beta$-hydrogen elimination. Instead of substitution of the protonated or methylated oxygen by $CH_3CN$, $Cl^-$or $I^-$, decomposition by $\beta$-hydrogen elimination from -$CH_2$-$CH_2$-OR (R = H, Me) seems to occur.

**Addition of a protonated 2-rhodaoxetane to acetonitrile**: Upon addition of a droplet of [$D_5$]pyridine to a solution of $\kappa^1$-*C*-2-hydroxyethyl complex [**5a**-$D_3$]$^{2+}$ in $CD_3CN$ (prepared by the reaction of [**3a**]$^+$ with $HBAr^f_4$ in $CD_3CN$, vide infra), [**5a**-$D_3$]$^{2+}$ rearranged to the metallacylic imino-ester [**8**-$D_3$]$^{2+}$ within 30 min (Scheme 6).

Clearly, the rearrangement of [**5a**]$^{2+}$ to [**8**]$^{2+}$ is base-catalysed. Imino-ester [**8**-$D_3$]$^{2+}$ could also be formed directly from [**3a**]$^+$: $^1$H NMR of a solution containing equimolar amounts of [**3a**]$BPh_4$ and $NH_4PF_6$ in $CD_3CN$ at room temperature revealed the quantitative formation of [**8**-$D_3$]$^{2+}$ via intermediate [**5a**-$D_3$]$^{2+}$ within 4 h. The undeuterated [**8**]$^{2+}$ was prepared analogously from [**3a**]$^+$ and $NH_4PF_6$ in $CH_3CN$, and was precipitated as pure [**8**]$(BPh_4)_2\cdot$MeOH by the addition of $NaBPh_4$ and MeOH.

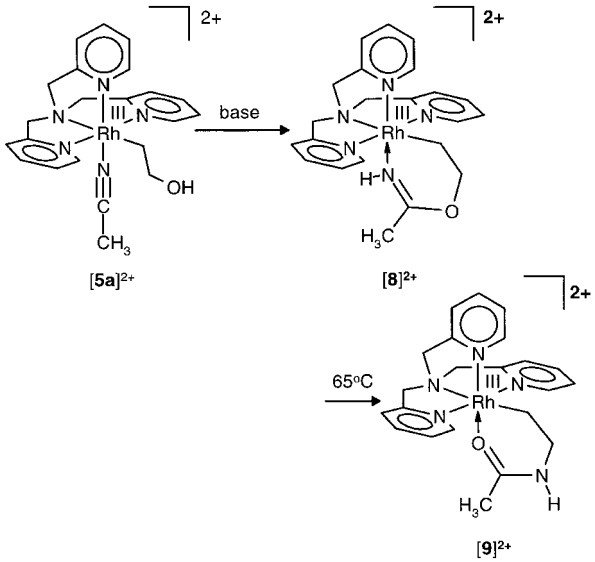


Scheme 6. Formation of 2-(acetimidoyloxy)ethyl complex [**8**]$^{2+}$ and 2-(acetylamino)ethyl complex [**9**]$^{2+}$ upon reaction of 2-rhoda(III)oxetane [**3a**]$^+$ with $NH_4PF_6$ in $CH_3CN$.

Thus, the reaction of [**3a**]$^+$ with $NH_4^+$/MeCN must proceed through the protonation of the 2-rhodaoxetane oxygen atom by $NH_4^+$, followed by reaction of [**4a**]$^{2+}$ with $CH_3CN$, to yield [**5a**]$^{2+}$ and $NH_3$. The ammonia subsequently facilitates the rearrangement of [**5a**]$^{2+}$ to imino ester [**8**]$^{2+}$, by the base-catalysed addition of the 2-hydroxyethyl group to the activated -C≡N bond of the coordinated $CH_3CN$,[26] analogous to a Pinner reaction [27] (Scheme 7, path a).

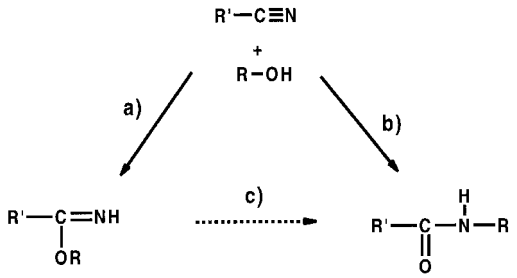


Scheme 7. Known reactivity of nitriles with alcohols in acidic media; path a) Pinner reaction; path b) Ritter reaction; path c) rearrangement of imidate to amide.

Crystals of [**8**]$(BPh_4)_2\cdot$MeOH, which were suitable for X-ray diffraction, were obtained by crystallisation from a saturated solution in DMSO, layered with MeOH. The crystal structure of [**8**]$^{2+}$ shows that the $\kappa^2$-*O*,*C*-2-oxyethyl fragment in [**3a**]$^+$ has been converted to a $\kappa^2$-*N*,*C*-2-(acetimidoyloxy)-ethyl fragment (Figure 6). Bond lengths for [**8**]$^{2+}$ are comparable to those reported for related $Rh^{III}$ and $Ir^{III}$ complexes.[28] The observed N5–$O_{MeOH}$ distance (3.04(3) Å) indicates N–H$\cdots O_{MeOH}$ hydrogen bonding.

Heating a solution of imino-ester [**8**]$(BPh_4)_2\cdot$MeOH in $CD_3CN$ or [$D_6$]DMSO to 65 °C resulted in the quantitative rearrangement of [**8**]$^{2+}$ to metallacyclic amide [**9**]$^{2+}$ within 3.5 h (Scheme 6). The lack of incorporation of $CD_3CN$ upon rearrangement of [**8**]$^{2+}$ to [**9**]$^{2+}$ in $CD_3CN$ demonstrates that the transformation is truly intramolecular. Both in $CD_3CN$ and in [$D_6$]DMSO, the rearrangement was found to be unaffected by the presence of $\leq$10 mol $H_2O$ per mol [**8**]$^{2+}$, thus showing that imino-ester [**8**]$^{2+}$ and amide [**9**]$^{2+}$ are both relatively stable towards hydrolysis. Amide [**9**]$^{2+}$ could also be formed directly from [**3a**]$^+$: $^1$H NMR spectra of a solution of equimolar amounts of [**3a**]$BPh_4$ and $NH_4PF_6$ in $CD_3CN$ at 65 °C revealed the quantitative conversion to the trideuterated amide [**9**-$D_3$]$^{2+}$ via the trideuterated imino-ester [**8**-$D_3$]$^{2+}$ within 4 h (Scheme 6). We obtained undeuterated [**9**]$^{2+}$ as crystalline [**9**]$(BPh_4)_2\cdot$MeCN by the analogous reaction in MeCN, followed by addition of $NaBPh_4$ (1 equiv) and partial evaporation of the solvent.

The crystal structure of [**9**]$(BPh_4)_2\cdot$MeCN confirms the rearrangement of the $\kappa^2$-*N*,*C*-2-(acetimidoyloxy)ethyl fragment in [**8**]$^{2+}$ to the $\kappa^2$-*O*,*C*-2-(acetylamino)ethyl fragment in [**9**]$^{2+}$ (Figure 6). Bond lengths observed for [**9**]$^{2+}$ are compa-

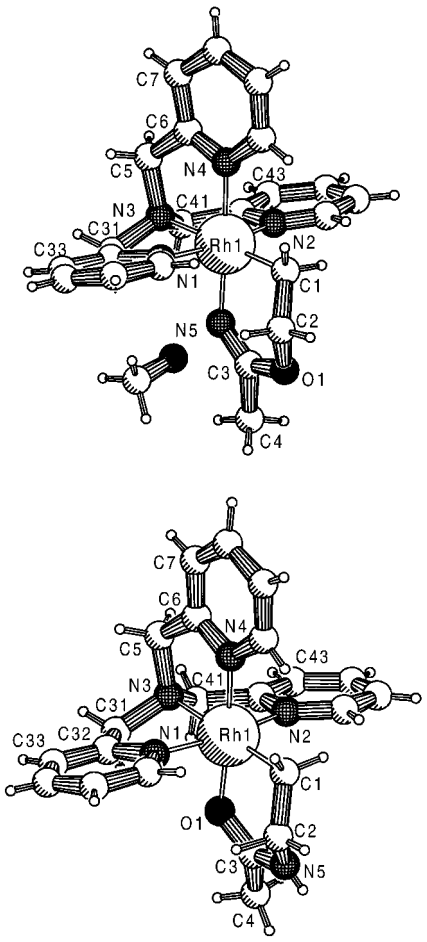


Figure 6. X-ray structures of 2-(acetimidoyloxy)ethyl complex $[\mathbf{8}]^{2+}\cdot$MeOH (top) and 2-(acetylamino)ethyl complex $[\mathbf{9}]^{2+}$ (bottom).

rable to those of other amide complexes of rhodium and iridium.[29]

The observed $\nu_{C=N}$ (1634 $cm^{-1}$) for $[\mathbf{8}]^{2+}$ and $\nu_{C=O}$ (1600 $cm^{-1}$) for $[\mathbf{9}]^{2+}$ are in accordance with their crystal structures. Selected NMR data for the Rh-$CH_2CH_2$-O-C(Me)=NH fragment of $[\mathbf{8}]^{2+}$ and the Rh-$CH_2CH_2$-NH-C(Me)=O fragment of $[\mathbf{9}]^{2+}$ are summarised in Tables 3 and 4. In the $^1$H NOESY spectrum, the acetimidoyl -NH- fragment of $[\mathbf{8}]^{2+}$ shows a clear NOE contact with the nearby axial protons of the two equivalent N-$CH_2$-Py fragments. The relatively small $^3J$(H,H) coupling constant between the Rh-$CH_2$- and the -$CH_2$-O- groups of $[\mathbf{8}]^{2+}$ (5.6 Hz) and $[\mathbf{9}]^{2+}$ (5.9 Hz) seems to be diagnostic for a six-membered metallacycle, in agreement with the value observed for cyclic chloro 2-hydroxyethyl complex $[\mathbf{6a}]^+$ in $CD_2Cl_2$ (5.3 Hz) for which we proposed a six-membered ring structure through intramolecular H-bonding (Scheme 5). Diagnostic for the conversion of $[\mathbf{8}]^{2+}$ to $[\mathbf{9}]^{2+}$ are the significant upfield shifts for -$CH_2$-N- in $[\mathbf{9}]^{2+}$ compared to -$CH_2$-O- in $[\mathbf{8}]^{2+}$ in the $^1$H NMR and $^{13}$C NMR spectra.

The overall rearrangement of intermediate $[\mathbf{5a}]^{2+}$ to $[\mathbf{9}]^{2+}$ is analogous to the Ritter reaction[27] (Scheme 7, path b). To the best of our knowledge, the conversion of the Pinner-type product $[\mathbf{8}]^{2+}$ to the Ritter-type product $[\mathbf{9}]^{2+}$, is an unprecedented example of rearrangement of an alkyl-alkanimidate to a *N*-alkyl alkanamide (see Scheme 7, path c: R,R′ = alkyl). Heating alkyl-alkanimidates generally results in the elimination of alcohols.[30] However, rearrangement of "activated" alkyl-trichloroacetimidates to *N*-alkyl trichloroacetamides, catalysed by $BF_3$, has been reported (Scheme 7, path c: R = alkyl, R′=$CCl_3$).[31] The mechanism proposed for this reaction involves formation of an ion-pair between the alkyl cation and the trichloroacetimidate (Scheme 8).

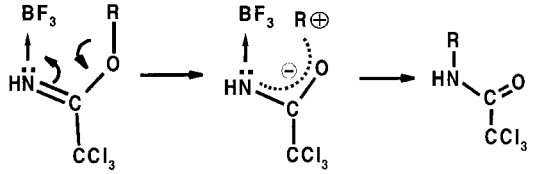


Scheme 8. Proposed mechanism for the $BF_3$-catalysed rearrangement of alkyl-trichloroacetimidates to *N*-alkyl trichloroacetamides.[31]

We propose that the mechanism for the transformation of $[\mathbf{8}]^{2+}$ to $[\mathbf{9}]^{2+}$ proceeds by the pathway shown in Scheme 9. $\beta$-Elimination of the acetimidato group gives an acetamidato–ethene complex which then reacts through migratory insertion of ethene into the Rh–N bond.

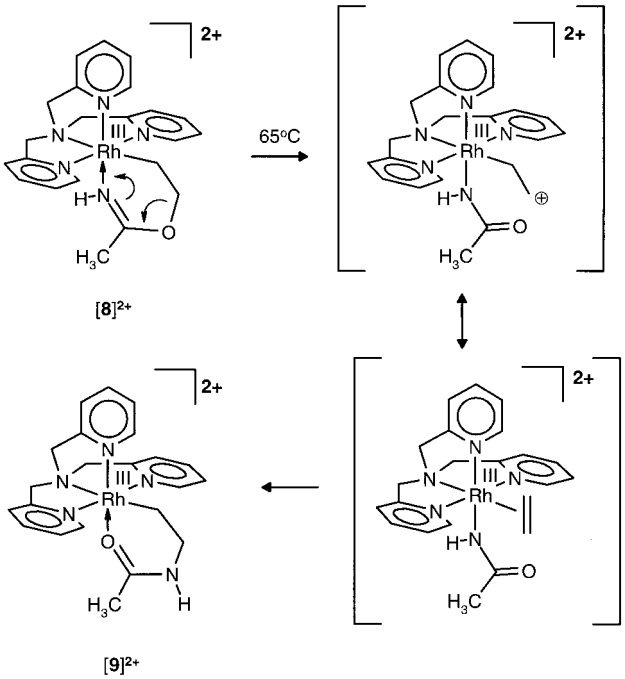


Scheme 9. Proposed mechanism for thermal rearrangement of $[\mathbf{8}]^{2+}$ to $[\mathbf{9}]^{2+}$.

Formation of a C–N bond from an olefin and an amine or amide is a very desirable transformation.[32] A catalytic version of this reaction would be a valuable alternative to classical industrial syntheses of amines or amides. However, the few catalytic examples of C–N bond formation reported to date are either slow or restricted to specific substrates or intramolecular reactions.[33] Therefore, new approaches to the formation of C–N bonds from olefins is of great interest. The step-wise conversion of ethene complex $[\mathbf{1a}]^+$ to a $\kappa^2$-*N*,*C*-2-



0947-6539/00/0601-0306 $ 17.50+.50/0 *Chem. Eur. J.* **2000**, *6*, No. 1

(acetylamino)ethyl complex $[\mathbf{9}]^{2+}$ via 2-rhodaoxetane $[\mathbf{3a}]^{+}$ (Scheme 10) is the first example of amidation of a coordinated olefin by $H_2O_2$, $H^+$ and a nitrile.

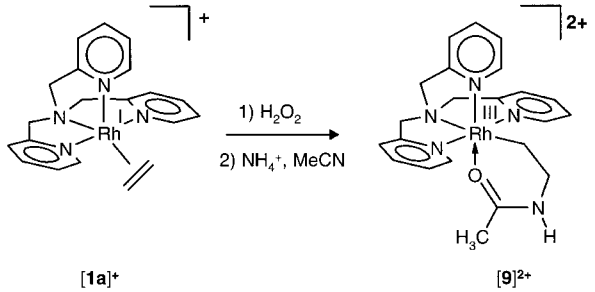


$[\mathbf{1a}]^{+}$ $[\mathbf{9}]^{2+}$

Scheme 10. Amidation of a coordinated olefin by $H_2O_2$, $H^+$ and MeCN.

**Addition of a 2-rhodaoxetane to acetone**: As observed by $^1$H NMR, a solution of 2-rhodaoxetane $[\mathbf{3a}]BPh_4$ in $[D_6]$acetone converts to the new metallacyclic ketal $[\mathbf{10}]^{+}$ in about two weeks (Scheme 11). The low $^3J$(H,H) coupling constant between the Rh-$CH_2$- and -$CH_2$-O fragments of $[\mathbf{10}]^{+}$, similar to those for $[\mathbf{8}]^{2+}$ and $[\mathbf{9}]^{2+}$, are in accordance with the presence of a six-membered metallacycle.

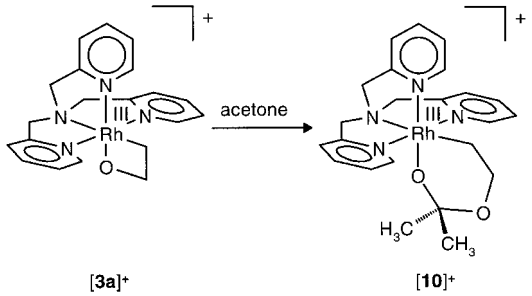


$[\mathbf{3a}]^{+}$ $[\mathbf{10}]^{+}$

Scheme 11. Reaction of $[\mathbf{3a}]^{+}$ with acetone to proposed complex $[\mathbf{10}]^{+}$.

A $^1$H NMR spectrum of a sample of $[\mathbf{10}]BPh_4$, isolated from non-deuterated acetone by precipitation with $Et_2O$, shows a singlet (relative integral 6H) at $\delta = 0.60$ in $[D_6]$acetone. This singlet disappears over a period of two days, and a signal of free $Me_2CO$ appears in the $^1$H NMR spectrum. All other signals of $[\mathbf{10}]^{+}$ remain unchanged. Apparently, the incorporated acetone exchanges for $[D_6]$acetone. As observed by $^1$H NMR spectroscopy, dissolution of $[\mathbf{10}]^{+}$ in solvents other than acetone results in the decomposition to a mixture of unidentified compounds. FAB-MS spectra, obtained from an acetone/*m*-nitrobenzyl alcohol matrix, were inconclusive because only $[(TPA)Rh]^{+}$ was detected as the highest mass. In view of the above-described reactivity of the 2-rhodaoxetanes induced by protonation, we assume that the reaction of $[\mathbf{3a}]^{+}$ with acetone is mediated by the acidity of this solvent.

## Conclusions

Despite their cationic nature, the pentacoordinate complexes $[(TPA)Rh^{I}(ethene)]^{+}$, $[\mathbf{1a}]^{+}$, and $[(MeTPA)Rh^{I}(ethene)]^{+}$, $[\mathbf{1b}]^{+}$, are clearly nucleophilic: they react with aqueous HCl to afford the chloro-ethyl complexes $[\mathbf{2a}]^{+}$–$[\mathbf{2c}]^{+}$.

Treatment of $[\mathbf{1a}]^{+}$ and $[\mathbf{1b}]^{+}$ with aqueous $H_2O_2$ results in the fast and selective oxygenation to the stable 2-rhodaoxetanes (1-oxa-2-rhodacyclobutanes) $[\mathbf{3a}]^{+}$ and $[\mathbf{3b}]^{+}$. These are the first isolated examples of unsubstituted 2-metallaoxetanes.

The 2-rhodaoxetanes obtained in this way are inert towards strong nucleophiles, such as $MeO^-$. The reactivity of the $\kappa^2$-*O*,*C*-2-oxyethyl fragments in the 2-rhodaoxetanes $[\mathbf{3a}]^{+}$ and $[\mathbf{3b}]^{+}$ is mainly determined by the nucleophilic character of their 2-rhodaoxetane oxygen. Reaction of $[\mathbf{3a}]^{+}$ and $[\mathbf{3b}]^{+}$ with $H^+$, converts the $\kappa^2$-*O*,*C*-2-oxyethyl fragment to a $\kappa^2$-*O*,*C*-2-hydroxyethyl fragment in the four-membered metallacycles $[\mathbf{4a}]^{2+}$ and $[\mathbf{4b}]^{2+}$. These eliminate acetaldehyde at room temperature in the absence of coordinating anions and coordinating solvents. The elimination of acetaldehyde from the unprotonated 2-rhodaoxetanes $[\mathbf{3a}]^{+}$ and $[\mathbf{3b}]^{+}$ only occurs at elevated temperatures. In both cases, the formation of ethylene-oxide is not observed.

The protonated 2-rhodaoxetane $[\mathbf{4a}]^{2+}$ undergoes ring-opening in the presence of MeCN or chloride anions to yield $[(TPA)Rh^{III}(\kappa^1$-*C*-2-hydroxyethyl)(MeCN)$]^{2+}$ ($[\mathbf{5a}]^{2+}$), or $[(TPA)Rh^{III}(\kappa^1$-*C*-2-hydroxyethyl)(Cl)$]^{+}$ ($[\mathbf{6a}]^{+}$), respectively. Similarly, reaction of $[\mathbf{3a}]^{+}$ with MeI results in the formation of $[(TPA)Rh^{III}(\kappa^1$-*C*-2-methoxyethyl)(I)$]^{+}$, $[\mathbf{7a}]^{+}$.

Reaction of $[\mathbf{3a}]^{+}$ with $NH_4^+$ in MeCN results in the formation of metallacyclic amide $[(TPA)Rh^{III}$(2-(acetylamino)ethyl)$]^{2+}$ ($[\mathbf{9}]^{2+}$) via the intermediate metallacyclic imino-ester $[(TPA)Rh^{III}$(2-(acetimidoyloxy)ethyl)$]^{2+}$ ($[\mathbf{8}]^{2+}$). The observed overall conversion of ethene complex $[\mathbf{1a}]^{+}$ to the metallacyclic amide $[\mathbf{9}]^{2+}$, via 2-rhodaoxetane $[\mathbf{3a}]^{+}$, provides a new step-wise route for the amidation of a metal-coordinated olefin fragment.

We have demonstrated that 2-metallaoxetanes readily form upon oxidation of a $Rh^{I}$(ethene) complex. This suggests their possible involvement in catalytic oxidation of olefins. Their role in the epoxidation of olefins, however, remains doubtful, despite frequently proposed mechanisms.[2]

Oxidative additions of epoxide C–O bonds to $Rh^{I}$, $Ni^0$, $Pd^0$, and $Pt^0$ complexes have been reported in stoichiometric and catalytic reactions.[5, 7a, 7b, 34–37] Furthermore, oxidative addition of ethylene oxide to $Ir^{I}$ has been reported to result in a *cis*-hydrido-formylmethyl $Ir^{III}$ complex.[24] The above examples, combined with the results in this paper, strongly suggest that, at least for late transition metals, the equilibrium between a 2-metallaoxetane and the reduced metal centre and epoxide is in favour of the 2-metallaoxetane. As a result, 2-metallaoxetanes do not decompose by reductive elimination but by other pathways, such as $\beta$-hydrogen elimination. In fact, formation of C–O bonds by reductive elimination from transition metal alkyl–alkoxide complexes is extremely rare.[38] There are some examples of the formation of $C_{aryl}$–O bonds in reasonable yields by oxidatively induced reductive elimination from $Ni^{II}$–aryl–alkoxide complexes and spontaneous reductive elimination from $Pd^{IV}$–aryl–alkoxide complexes.[39] Oxidatively induced reductive eliminations of cyclic ethers (e. g. THF) from oxametallacyclic $Ni^{II}$–alkyl–alkoxide complexes have only been realised in very low yields.[40] Elimination of an epoxide from a 2-oxametallacyclobutane (2-metallaoxetane) would not only involve the apparently

unfavourable reductive elimination of a C–O bond, but also the formation of a strained epoxide from a less strained oxametallacyclobutane. The direct reductive elimination of epoxides from detectable 2-metallaoxetanes will therefore be thermodynamically too "uphill". 2-Rhodaoxetanes could, however, be involved as intermediates in rhodium-catalysed oxidation of terminal olefins to methylketones by alkylhydroperoxides, hydrogen peroxide or $O_2$.[41]

## Experimental Section

**General methods**: All procedures were performed under $N_2$ using standard Schlenk techniques. Solvents (p. a.) were deoxygenated by bubbling a stream of $N_2$ through them or by the freeze-pump-thaw method. "Room temperature" corresponds to $\approx 20\,^{\circ}C$.

IR spectra were measured on a Perkin–Elmer 1720X. NMR experiments were carried out on a Bruker DPX200 (200 MHz and 50 MHz for $^1H$ and $^{13}C$, respectively), a Bruker AC300 (300 MHz and 75 MHz for $^1H$ and $^{13}C$, respectively) and a Bruker WM400 (400 MHz and 100 MHz for $^1H$ and $^{13}C$, respectively). Solvent shift reference for $^1H$ NMR: [D$_6$]acetone $\delta(^1H) = 2.05$, $CD_3CN$ $\delta(^1H) = 1.98$, $CD_2Cl_2$ $\delta(^1H) = 5.31$, [D$_6$]DMSO $\delta(^1H) = 2.50$. For $^{13}C$ NMR: [D$_6$]acetone $\delta(^{13}C) = 29.50$, $CD_3CN$ $\delta(^{13}C) = 1.28$, $CD_2Cl_2$ $\delta(^{13}C) = 54.20$, [D$_6$]DMSO $\delta(^{13}C) = 39.50$. Abbreviations used are s = singlet, d = doublet, dd = doublet of doublets, t = triplet, dt = doublet of triplets, q = quartet, dq = doublet of quartets, m = multiplet and br = broad. Elemental analysis (C, H, N) were carried out on a Carlo Erba NCSO-analyser. Mass Spectra (FAB) were recorded on a VG 7070 mass spectrometer or on a JEOL JMS SX/SX102A four-sector mass spectrometer.

$[\{(C_2H_4)_2Rh(\mu\text{-}Cl)\}_2]$,[42] and the ligands TPA[43] and MeTPA[44] were prepared according to literature procedures. All other chemicals are commercially available and were used without further purification, unless stated otherwise.

**X-ray diffraction**: For all structures, single crystals were mounted in air on glass fibres. Intensity data were collected on an Enraf-Nonius CAD4 diffractometer (radiation: graphite monochromatised $Cu_{K\alpha} = 1.541838$ Å). Intensity data were corrected for Lorentz and polarisation effects. Semi-empirical absorption correction ($\psi$-scan)[45] was applied. The structures were solved by the program system DIRDIF[46] with the program PATTY[47] to locate the heavy atoms and were refined with standard methods (refinement against $F^2$ for all reflections with SHELXL97[48] with anisotropic parameters for the non-hydrogen atoms. Selected bond lengths and angles are summarised in Tables 1 and 2. Other relevant crystal data are summarised in Table 5. Drawings were generated with the program PLATON.[49]

**[1b]BPh$_4$, [2b]BPh$_4$ and [3b]BPh$_4$·1.5H$_2$O**: The hydrogen atoms of the methyl groups were refined as rigid rotors with idealised $sp^3$ hybridisation and a C–H bond length of 0.97 Å to match maximum electron density in a difference Fourier map. All other hydrogens were initially placed at calculated positions and were then freely refined.

**[2c]BPh$_4$**: The hydrogen atoms of the methyl groups were refined as rigid rotors with idealised $sp^3$ hybridisation and a C–H bond length of 0.97 Å to match maximum electron density in a difference Fourier map. The

Table 5. Crystallographic data of the synthesised complexes

| | [**1b**]BPh$_4$ | [**2b**]BPh$_4$ | [**2c**]BPh$_4$ | [**3b**]BPh$_4$·1.5H$_2$O | [**6a**]BPh$_4$·MeOH | [**8**](BPh$_4$)$_2$·MeOH | [**9**](BPh$_4$)$_2$·MeCN |
|---|---|---|---|---|---|---|---|
| empirical formula | $C_{45}H_{44}N_4BRh$ | $C_{45}H_{45}N_4BClRh$ | $C_{45}H_{45}N_4BClRh$ | $C_{45}H_{44}N_4O_{2.5}BRh$ | $C_{45}H_{47}N_4O_2BClRh$ | $C_{71}H_{70}N_5O_2B_2Rh$ | $C_{72}H_{69}N_6OB_2Rh$ |
| crystal size [mm] | 0.25 × 0.13 × 0.06 | 0.56 × 0.34 × 0.12 | 0.36 × 0.25 × 0.13 | 0.56 × 0.34 × 0.18 | 0.46 × 0.36 × 0.29 | 0.38 × 0.09 × 0.06 | 0.27 × 0.18 × 0.10 |
| formula weight | 754.56 | 791.02 | 981.02 | 794.56 | 825.04 | 1149.85 | 1158.86 |
| $T$ [K] | 208(2) | 208(2) | 208(2) | 173(2) | 208(2) | 208(2) | 293(2) |
| crystal system | triclinic | orthorhombic | monoclinic | triclinic | monoclinic | monoclinic | monoclinic |
| space group | $P\bar{1}$ | $Pbc2_1$ | $P2_1/c$ | $P\bar{1}$ | $P2_1/c$ | $C2/c$ | $C2/c$ |
| unit cell dim. from $N$ refl. | 23 | 10 | 24 | 10 | 8 | 16 | 15 |
| $a$ [Å] | 9.843(4) | 10.6840(16) | 14.4306(5) | 9.3022(3) | 13.86(2) | 37.334(7) | 28.270(2) |
| $b$ [Å] | 11.52(2) | 18.960(5) | 9.8390(6) | 11.8120(2) | 10.155(9) | 12.8324(18) | 23.0952(14) |
| $c$ [Å] | 16.87(2) | 37.402(7) | 27.5464(13) | 18.3852(4) | 28.752(4) | 24.767(5) | 21.520(2) |
| $\alpha$ [°] | 88.54(12) | 90 | 90 | 78.781(5) | 90 | 90 | 90 |
| $\beta$ [°] | 76.60(12) | 90 | 94.757(4) | 88.275(3) | 95.56(3) | 97.37(2) | 119.793(6) |
| $\gamma$ [°] | 82.15(10) | 90 | 90 | 85.428(3) | 90 | 90 | 90 |
| $V$ [Å$^3$] | 1843(4) | 7577(3) | 3897.6(3) | 1974.99(8) | 4029(7) | 11767(4) | 12192.9(16) |
| $\rho_{calcd}$ [g cm$^{-3}$] | 1.360 | 1.387 | 1.348 | 1.336 | 1.360 | 1.298 | 1.263 |
| $Z$ | 2 | 8 | 4 | 2 | 4 | 8 | 8 |
| diffractometer | Enraf-Nonius CAD4 | Enraf-Nonius CAD4 | Enraf-Nonius CAD4 | Enraf-Nonius CAD4 | Enraf-Nonius CAD4 | Enraf-Nonius CAD4 | Enraf-Nonius CAD4 |
| scan | $\theta-2\theta$ | $\omega$ | $\theta-2\theta$ | $\theta-2\theta$ | $\theta-2\theta$ | $\omega$ | $\theta-2\theta$ |
| radiation | $Cu_{K\alpha}$ | $Cu_{K\alpha}$ | $Cu_{K\alpha}$ | $Cu_{K\alpha}$ | $Cu_{K\alpha}$ | $Cu_{K\alpha}$ | $Cu_{K\alpha}$ |
| wavelength [Å] | 1.54184 | 1.54184 | 1.54184 | 1.54184 | 1.54184 | 1.54184 | 1.54184 |
| $F(000)$ | 784 | 3280 | 1640 | 824 | 1712 | 4816 | 4848 |
| $\theta$ range [°] | 3.88–70.27 | 4.66–69.98 | 3.07–69.97 | 3.83–70.03 | 3.09–70.09 | 4.00–55.24 | 2.88–69.96 |
| index ranges | $-11 \le h \le 0$ | $-13 \le h \le 0$ | $-17 \le h \le 17$ | $0 \le h \le 11$ | $-16 \le h \le 0$ | $-39 \le h \le 39$ | $-34 \le h \le 29$ |
| | $-14 \le k \le 13$ | $-23 \le k \le 0$ | $-11 \le k \le 0$ | $-14 \le k \le 14$ | $0 \le k \le 12$ | $-13 \le k \le 0$ | $0 \le k \le 28$ |
| | $-20 \le l \le 19$ | $0 \le l \le 45$ | $-33 \le l \le 0$ | $-22 \le l \le 22$ | $-34 \le l \le 35$ | $0 \le l \le 26$ | $0 \le l \le 26$ |
| range of rel. transm. fac. | 0.714/1.215 | 0.807/1.777 | 0.802/1.297 | 1.210/0.910 | 0.843/1.186 | 0.944/1.065 | 1.081/0.924 |
| measured reflections | 7404 | 7281 | 7520 | 7987 | 7956 | 7588 | 11863 |
| unique reflections | 6970 | 7281 | 7353 | 7492 | 7625 | 7374 | 11535 |
| observed reflections $[I_o > 2\sigma(I_o)]$ | 5417 | 6107 | 6269 | 6908 | 6027 | 2886 | 6778 |
| refined parameters | 462 | 941 | 619 | 727 | 473 | 732 | 993 |
| goodness-of-fit on $F^2$ | 1.054 | 1.077 | 1.057 | 1.076 | 1.093 | 1.020 | 1.041 |
| $R$ $[I_o > 2\sigma(I_o)]$ | 0.0855 | 0.1040 | 0.0501 | 0.0566 | 0.0992 | 0.0877 | 0.0552 |
| $wR2$ [all data] | 0.2373 | 0.3380 | 0.1330 | 0.1786 | 0.2774 | 0.1794 | 0.1255 |
| final residual electron density (max/min) [e Å$^{-3}$] | 3.403/−3.786 | 4.011/−3.573 | 0.712/−2.140 | 2.203/−0.588 | 1.959/−2.072 | 0.456/−0.464 | 0.587/−0.621 |



0947-6539/00/0601-0308 $ 17.50+.50/0 *Chem. Eur. J.* **2000**, *6*, No. 1

hydrogen atoms attached to C1 were placed at calculated positions and were refined riding on the parent atom. All other hydrogens were initially placed at calculated positions and were then freely refined.

**[8](BPh$_4$)$_2$·MeOH and [9](BPh$_4$)$_2$·CH$_3$CN**: The hydrogen atoms of the methyl groups were refined as rigid rotors with idealised sp$^3$ hybridisation and a C–H bond length of 0.97 Å to match maximum electron density in a difference Fourier map. The hydrogen atom attached to the nitrogen atom in [**9**]$^{2+}$ was taken from a difference Fourier map. In contrast to the structure analysis of [**9**](BPh$_4$)$_2$·CH$_3$CN, the presence of a nitrogen atom at the N5 position in [**8**]$^{2+}$ is not unambiguously confirmed by the localisation of an attached proton. However, during refinement it became clear that only the presented structure shows acceptable ADP values for N5 and O1. All other hydrogens were initially placed at calculated positions and were then freely refined.

Crystallographic data (excluding structure factors) for the structures reported in this paper have been deposited with the Cambridge Crystallographic Data Centre as supplementary publication nos. CCDC-117405 ([**1b**]BPh$_4$), CCDC-117406 ([**2b**]BPh$_4$), CCDC-117407 ([**2c**]BPh$_4$), CCDC-117408 ([**3b**]BPh$_4$·1.5H$_2$O), CCDC-117409 ([**6a**]BPh$_4$·MeOH), CCDC-117410 ([**8**](BPh$_4$)$_2$·MeOH) and CCDC-117411 ([**9**](BPh$_4$)$_2$·MeOH). Copies of the data can be obtained free of charge on application to CCDC, 12 Union Road, Cambridge CB2 1EZ, UK (fax: (+44) 1223-336-033; e-mail: deposit@ccdc.cam.ac.uk).

**($\eta^2$-Ethene)-($\kappa^4$-*N,N,N*-tri-(2-pyridylmethyl)amine)-rhodium(I) hexafluorophosphate/tetrafluoroborate ([1a]PF$_6$) and ([1a]BF$_4$)**: [{(C$_2$H$_4$)$_2$Rh($\mu$-Cl)}$_2$] (100 mg, 0.26 mmol) and TPA (150 mg, 0.52 mmol) were stirred in MeOH (25 mL) at −78 °C for 1 h followed by the addition of KPF$_6$ (441 mg, 2.4 mmol). Partial evaporation of the solvent caused the precipitation of [**1a**]PF$_6$ as a yellow powder, which was filtered and vacuum-dried. Yield: 68 % (200 mg). The same procedure with NaBF$_4$ gave [**1a**]BF$_4$ (yield: 71 %).

In both the $^1$H and the $^{13}$C NMR spectra of [**1a**]$^+$ at 298 K, the ethene fragment is observed as two broad singlets. At 263 K the ethene fragment is observed as two pseudo double-triplets in the $^1$H NMR spectrum and two doublets in the $^{13}$C NMR spectrum. $^1$H NMR (500.14 MHz, [D$_6$]acetone, 263 K): $\delta$ = 9.43 (d, $^3J$(H,H) = 4.7 Hz, 1H; Py$_a$-H6), 8.16 (d, 2H, $^3J$(H,H) = 5.8 Hz, 2H; Py$_b$-H6), 7.90–7.10 (m, 9H; Py-H4, Py-H5 and Py-H3), 5.69 (d[AB], $^2J$(H,H) = 15.6 Hz, 2H; N-CH$_2$-Py$_b$), 5.02 (d[AB], $^2J$(H,H) = 15.6 Hz, 2H; N-CH$_2$-Py$_b$), 4.76 (s, 2H; N-CH$_2$-Py$_a$), 2.11 (dt, average $J$(H,H) = 9.5 Hz, $J$(H,H) or $J$(H,Rh) = 1.7 Hz, 2H; C$_2$H$_4$), 1.82 (dt, $J$(H,H) = 9.5 Hz, $J$(H,H) or $J$(Rh,H) = 1.7 Hz, 2H; C$_2$H$_4$); $^{13}$C{$^1$H} NMR (125.77 MHz, [D$_6$]acetone, 263 K): $\delta$ = 163.9 (Py$_b$-C2), 159.6 (Py$_a$-C2), 151.9 (Py$_a$-C6), 151.4 (Py$_b$-C6), 138.1 (Py$_a$-C4), 137.3 (Py$_b$-C4), 125.2 (Py$_b$-C3), 124.4 (Py$_a$-C3), 123.1 (Py$_b$-C5), 122.2 (Py$_a$-C5), 69.6 (N-CH$_2$-Py$_b$), 64.3 (N-CH$_2$-Py$_a$), 27.2 (d, $J$(C,Rh) = 18.0 Hz; C=C), 25.0 (d, $J$(C,Rh) = 19.7 Hz; C=C); FAB-MS (m-nitrobenzyl alcohol matrix (*m*-Noba)/CH$_3$CN): 589 [(Na+*M*+PF$_6$)$^+$], 421 [*M*$^+$], 393 [(*M* − C$_2$H$_4$)$^+$]; anal. calcd for [**1a**]PF$_6$ (C$_{20}$H$_{22}$N$_4$RhPF$_6$): C 42.42, H 3.93, N 9.98; found: C 40.54, H 3.60, N 9.70; anal. calcd for [**1a**]BF$_4$ (C$_{20}$H$_{22}$N$_4$RhBF$_4$): C 47.28, H 4.36, N 11.03; found: C 47.25, H 4.46, N 10.80.

**($\eta^2$-Ethene)-($\kappa^4$-*N*-[(6-methyl-2-pyridyl)methyl]-*N,N*-di(2-pyridylmethyl)-amine)-rhodium(I) tetraphenylborate ([1b]BPh$_4$)**: [{(C$_2$H$_4$)$_2$Rh($\mu$-Cl)}$_2$] (200 mg, 0.51 mmol) and MeTPA (320 mg, 1.05 mmol) were added to MeOH (25 mL) at −78 °C, and stirred for 1 h. Any undissolved material was removed by filtration. NaBPh$_4$ (360 mg, 1.06 mmol) in MeOH (7 mL) was added to the solution. The yellow solid which precipitated was collected by filtration. Crystals suitable for X-ray diffraction were obtained by slow crystallisation of a saturated solution of [**1b**]BPh$_4$ in acetone at −20 °C. Yield: 81 % (623 mg); $^1$H NMR (200.13 MHz, CD$_2$Cl$_2$, 298 K): $\delta$ = 7.86 (d, $^3J$(H,H) = 5.3 Hz, 2H; Py$_a$-H6), 7.55–6.65 (m, 9H; Py-H4, Py-H5 and Py-H3), 7.37 (m, 8H; BAr-H2), 7.02 (t, $^3J$(H,H) = 7.4 Hz, 8H; BAr-H3), 6.87 (t, $^3J$(H,H) = 7.4 Hz, 4H; BAr-H4), 5.07 (d[AB], $^2J$(H,H) = 15.3 Hz, 2H; N-CH$_2$-Py$_b$), 4.23 (d[AB], $^2J$(H,H) = 15.3 Hz, 2H; N-CH$_2$-Py$_b$), 4.11 (s, 2H; N-CH$_2$-Py$_a$), 3.33 (s, 3H; Py$_a$-CH$_3$), 2.07 (br s, 2H; C$_2$H$_4$), 1.94 (br s, 2H; C$_2$H$_4$); $^{13}$C{$^1$H} NMR (125.77 MHz, CD$_2$Cl$_2$, 298 K): $\delta$ = 164.8 (q, $^1J$(C,B) = 49.5 Hz; BAr-C1), 163.3 (Py$_b$-C2), 161.2 (Py$_a$-C2), 158.0 (Py$_a$-C6), 151.3 (Py$_b$-C6), 138.3 (Py$_a$-C4), 137.3 (Py$_b$-C4), 136.8 (BAr-C2), 126.5 (q, $^3J$(C,B) = 2.8 Hz; BAr-C3), 125.3 (Py$_b$-C3), 124.4 (Py$_a$-C3), 123.1 (Py$_b$-C5), 122.7 (BAr-C4), 119.2 (Py$_a$-C5), 69.8 (N-CH$_2$-Py$_b$), 65.3 (N-CH$_2$-Py$_a$), 30.6 (br s, C=C), 29.1 (Py$_a$-CH$_3$), 26.3 (br s, C=C); FAB-MS (*m*-Noba/CH$_3$CN): 435 [*M*$^+$], 407 [(*M* − C$_2$H$_4$)$^+$]; anal. calcd for C$_{45}$H$_{44}$N$_4$BRh: C 71.63, H 5.88, N 7.42; found: C 71.15, H 5.93, N 7.42.

**(Ethyl)-(chloro)-($\kappa^4$-*N,N,N*-tri(2-pyridylmethyl)amine)-rhodium(III) hexafluorophosphate ([2a]PF$_6$)**: [{(C$_2$H$_4$)$_2$Rh($\mu$-Cl)}$_2$] (150 mg, 0.38 mmol) and TPA (320 mg, 1.1 mmol) were added to MeOH (40 mL) at −78 °C, and stirred for 1 h. An aqueous solution of HCl (0.4 mL, 30 %) was added and the solution was allowed to slowly warm to −10 °C (within 2 h). Any undissolved material was removed by filtration. NaPF$_6$ (740 mg, 4.40 mmol) in MeOH (7 mL) was added to the solution. The light yellow solid which precipitated was collected by filtration. Yield: 71 % (325 mg); $^1$H NMR (200.13 MHz, [D$_6$]acetone, 298 K): $\delta$ = 9.40 (d, 1H, $^3J$(H,H) = 4.7 Hz, Py$_a$-H6), 8.89 (d, 2H, $^3J$(H,H) = 5.6 Hz, Py$_b$-H6), 8.0–7.37 (m, 9H, Py-H4, Py-H5 and Py-H3), 5.40 (d[AB], 2H, $^3J$(H,H) = 16.2 Hz, N-CH$_2$-Py$_b$), 5.07 (s, 2H, N-CH$_2$-Py$_a$), 5.03 (dd[AB], 2H, $^3J$(H,H) = 16.2 Hz, $^3J$(Rh,H) = 1.5 Hz, N-CH$_2$-Py$_b$), 2.71 (dq, 2H, $^3J$(H,H) = 7.4 Hz, $^2J$(Rh,H) = 2.7 Hz, Rh-CH$_2$CH$_3$), 0.61 (t, 3H, $^3J$(H,H) = 7.4 Hz, Rh-CH$_2$CH$_3$); $^{13}$C{$^1$H} NMR (50.33 MHz, [D$_6$]acetone, 298 K): $\delta$ = 162.9 (Py$_b$-C2), 158.0 (Py$_a$-C2), 151.4 (Py$_b$-C6), 149.0 (Py$_a$-C6), 139.2 (Py$_b$-C4), 139.0 (Py$_a$-C4), 125.7 (Py$_b$-C3), 125.1 (Py$_a$-C3), 123.8 (Py$_b$-C5), 121.4 (Py$_a$-C5), 72.2 (N-CH$_2$-Py$_a$), 69.3 (N-CH$_2$-Py$_b$), 16.9 (Rh-CH$_2$CH$_3$), 15.4 (d, $^1J$(C,Rh) = 21.9 Hz, Rh-CH$_2$CH$_3$); FAB-MS (*m*-Noba/CH$_3$CN): *m*/*z*: 457 [*M* − PF$_6$]$^+$, 428 [*M* − CH$_2$CH$_3$ − PF$_6$]$^+$, 393 [*M* − CH$_2$CH$_3$ − PF$_6$ − Cl]$^+$; anal. calcd for [**2a**]$^+$, (C$_{20}$H$_{23}$N$_4$RhCl): 457.0683; found: 457.0666.

**(Ethyl)-(chloro)-($\kappa^4$-*N*-[(6-methyl-2-pyridyl)methyl]-*N,N*-di(2-pyridylmethyl)amine)-rhodium(III) tetraphenylborate ([2b]BPh$_4$)**: [{(C$_2$H$_4$)$_2$Rh($\mu$-Cl)}$_2$] (100 mg, 0.26 mmol) and MeTPA (160 mg, 0.53 mmol) were added to MeOH (25 mL) at −78 °C, and stirred for 1 h. An aqueous solution of HCl (0.4 mL, 30 %) was added and the solution was allowed to slowly warm to −10 °C (within ≈2 h). Any undissolved material was removed by filtration. NaBPh$_4$ (360 mg, 1.06 mmol) in MeOH (7 mL) was added to the solution. The light yellow solid which precipitated was collected by filtration. After recrystallisation from a saturated CH$_3$CN solution, pure [**2b**]BPh$_4$ was obtained as bright yellow crystals which were suitable for X-ray diffraction. Yield: 60 % (244 mg); $^1$H NMR (200.13 MHz, CD$_2$Cl$_2$, 298 K): $\delta$ = 8.80 (d, 2H, $^3J$(H,H) = 5.9 Hz, Py$_b$-H6), 7.8–6.6 (m, 9H, Py-H4, Py-H5 and Py-H3), 7.46 (m, 8H, BAr-H2), 7.05 (t, 8H, $^3J$(H,H) = 7.3 Hz, BAr-H3), 6.89 (t, 4H, $^3J$(H,H) = 7.3 Hz, BAr-H4), 4.09 (d[AB], 2H, $^3J$(H,H) = 16.2 Hz, N-CH$_2$-Py$_b$), 3.59 (s, 2H, N-CH$_2$-Py$_a$), 3.36 (dd[AB], 2H, $^3J$(H,H) = 16.2 Hz, $^3J$(Rh,H) = 1.5 Hz, N-CH$_2$-Py$_b$), 3.02 (s, 3H, Py$_a$-CH$_3$), 2.71 (dq, 2H, $^3J$(H,H) = 7.4 Hz, $^2J$(Rh,H) = 2.7 Hz, Rh-CH$_2$CH$_3$), 0.36 (t, 3H, $^3J$(H,H) = 7.4 Hz, Rh-CH$_2$CH$_3$); $^{13}$C{$^1$H} NMR (50.33 MHz, CD$_2$Cl$_2$, 298 K): $\delta$ = 164.9 (q, $^1J$(C,B) = 49.5 Hz; BAr-C1), 164.3 (Py$_a$-C2), 162.5 (Py$_b$-C2), 154.9 (Py$_a$-C6), 152.3 (Py$_b$-C6), 139.3 (Py$_b$-C4), 139.0 (Py$_a$-C4), 136.8 (BAr-C2), 126.7 (q, $^3J$(C,B) = 2.8 Hz; BAr-C3, Py$_a$-C3), 125.7 (Py$_b$-C3), 123.6 (Py$_b$-C5), 122.9 (BAr-C4), 119.8 (Py$_a$-C5), 71.4 (N-CH$_2$-Py$_a$), 67.7 (N-CH$_2$-Py$_b$), 26.3 (Py$_a$-CH$_3$), 20.9 (d, $^1J$(C,Rh) = 23.6 Hz, Rh-CH$_2$CH$_3$), 17.8 (Rh-CH$_2$CH$_3$); FAB-MS (*m*-Noba/CH$_3$CN): *m*/*z*: 471 [*M* − BPh$_4$]$^+$, 428 [*M* − CH$_2$CH$_3$ − BPh$_4$]$^+$, 407 [*M* − CH$_2$CH$_3$ − BPh$_4$ − Cl]$^+$; anal. calcd for [**2b**]BPh$_4$, (C$_{45}$H$_{45}$N$_4$RhClB): C 68.33, H 5.73, N 7.08; found: C 68.65, H 5.34, N 7.09.

**(Ethyl)-(chloro)-($\kappa^4$-*N*-[(6-methyl-2-pyridyl)methyl]-*N,N*-di(2-pyridylmethyl)amine)-rhodium(III) tetraphenylborate ([2c]BPh$_4$)**: [{(C$_2$H$_4$)$_2$Rh($\mu$-Cl)}$_2$] (200 mg, 0.51 mmol) and MeTPA (320 mg, 1.05 mmol) were added to MeOH (25 mL) at −78 °C, and stirred for 1 h. An aqueous solution of HCl (0.1 mL, 30 %) was added and the solution was allowed to warm to room temperature (within 30 min) by the removal of the acetone/CO$_2$ bath. Any undissolved material was removed by filtration. NaBPh$_4$ (640 mg, 1.87 mmol) in MeOH (7 mL) was added to the solution. The orange solid which precipitated was collected by filtration. After recrystallisation from a saturated CH$_3$CN solution, pure [**2c**]BPh$_4$ was obtained as bright orange crystals which were suitable for X-ray diffraction. Yield: 63 % (510 mg); $^1$H NMR (200.13 MHz, CD$_2$Cl$_2$, 298 K): $\delta$ = 9.35 (d, 1H, $^3J$(H,H) = 5.3 Hz, Py$_a$-H6), 8.88 (d, 1H, $^3J$(H,H) = 5.9 Hz, Py$_b$-H6), 7.8–6.8 (m, 9H, Py-H4, Py-H5 and Py-H3), 7.46 (m, 8H, BAr-H2), 7.05 (t, 8H, $^3J$(H,H) = 7.3 Hz, BAr-H3), 6.89 (t, 4H, $^3J$(H,H) = 7.3 Hz, BAr-H4), 4.40 (d[AB], 1H, $^3J$(H,H) = 15.6 Hz, N-CH$_2$-Py), 4.13 (d[AB], 1H, $^3J$(H,H) = 16.5 Hz, N-CH$_2$-Py), 3.76 (d[AB], 1H, $^3J$(H,H) = 17.3 Hz, N-CH$_2$-Py), 3.60 (d[AB], 1H, $^3J$(H,H) = 17.3 Hz, N-CH$_2$-Py), 3.52 (d[AB], 1H, $^3J$(H,H) = 15.6 Hz, N-CH$_2$-Py), 3.32 (d[AB], 1H, $^3J$(H,H) = 16.5 Hz, N-CH$_2$-Py), 2.85 (s, 3H, Py$_c$-CH$_3$), 2.79 (m, 1H, Rh-CH$_a$H$_b$CH$_3$), 2.56 (m, 1H, Rh-CH$_a$H$_b$CH$_3$), 0.56 (t, 3H, $^3J$(H,H) = 7.4 Hz, Rh-CH$_2$CH$_3$); $^{13}$C{$^1$H} NMR

(50.33 MHz, $CD_2Cl_2$, 298 K): $\delta = 164.9$ (q, $^1J(C,B) = 49.5$ Hz; BAr-C1), 166.5, 162.3, 161.5 ($Py_a$-C2, $Py_b$-C2, $Py_C$-C2), 156.9 ($Py_c$-C6), 151.0, 150.0 ($Py_a$-C6, $Py_b$-C6), 139.4, 139.2, 139.0 ($Py_a$-C4, $Py_b$-C4, $Py_c$-C4), 136.8 (BAr-C2), 126.7 (q, $^3J(C,B) = 2.8$ Hz; BAr-C3), 127.3, 125.6, 125.3 ($Py_a$-C3, $Py_b$-C3, $Py_c$-C3), 122.9 (BAr-C4), 122.7, 121.9, 121.0 ($Py_a$-C5, $Py_b$-C5, $Py_c$-C5), 71.4 (N-$CH_2$-Py), 69.6 (N-$CH_2$-Py), 69.0 (N-$CH_2$-Py), 28.3 ($Py_a$-$CH_3$), 17.8 (Rh-$CH_2CH_3$), 17.5 (d, $^1J(C,Rh) = 20.4$ Hz, Rh-$CH_2CH_3$); FAB-MS (*m*-Noba/$CH_3CN$): *m*/*z*: 471 $[M - BPh_4]^+$, 428 $[M - CH_2CH_3 - BPh_4]^+$, 407 $[M - CH_2CH_3 - BPh_4 - Cl]^+$; anal. calcd for [**2c**]$BPh_4$, ($C_{45}H_{45}N_4RhClB$): C 68.33, H 5.73, N 7.08; found: C 68.19, H 5.27, N 7.06.

**($\kappa^2$-*O,C*-2-Oxyethyl)-($\kappa^4$-*N,N,N*-tri(2-pyridylmethyl)amine)-rhodium(III) hexafluorophosphate/tetraphenylborate ([3a]$PF_6$ and [3a]$BPh_4$)**: [**1a**]$PF_6$ (50 mg, 0.088 mmol) was dissolved in MeOH (5 mL) and an aqueous solution of $H_2O_2$ (0.1 mL, 35 %) was added. The solution was stirred at $-10\,^\circ C$ for 1 h. Addition of $Et_2O$ caused the precipitation of [**3a**]$PF_6$ as a pale-yellow powder, which was filtered, washed with $Et_2O$, and vacuum dried. Yield: 100 % (51 mg).

**[3a]($BPh_4$)**: This compound was obtained by in situ oxidation of [**1a**]Cl: $[\{(C_2H_4)_2Rh(\mu\text{-}Cl)\}_2]$ (100 mg, 0.25 mmol) and TPA (150 mg, 0.52 mmol) were stirred in MeOH (25 mL) at $-78\,^\circ C$ for 1 h. An aqueous solution of $H_2O_2$ (0.12 mL, 35 %) was added and the mixture was allowed to slowly warm to room temperature Any undissolved material was removed by filtration. $NaBPh_4$ (180 mg, 0.53 mmol) in MeOH (7 mL) was added to the solution. The light yellow solid which precipitated was collected by filtration. Yield: 60 % (240 mg); $^1H$ NMR (200.13 MHz, [$D_6$]acetone, 298 K): $\delta = 9.03$ (d, $^3J(H,H) = 5.7$ Hz, 2H; $Py_b$-H6), 8.70 (d, $^3J(H,H) = 5.5$ Hz, 1H; $Py_a$-H6), 8.10–7.20 (m, 9H; Py-H4, Py-H5 and Py-H3), 5.32 (d[AB], $^2J(H,H) = 15.4$ Hz, 2H; N-$CH_2$-$Py_b$), 5.13 (d[AB], $^2J(H,H) = 15.4$ Hz, 2H; N-$CH_2$-$Py_b$), 5.04 (s, 2H; N-$CH_2$-$Py_a$), 4.97 (t, $^3J(H,H) = 7.5$ Hz, 2H; Rh-$CH_2CH_2$O-), 2.90 (s, ≈3H; $H_2O$), 2.35 (dt, $^3J(H,H) = 7.5$ Hz, $^2J(H,Rh) = 2.5$ Hz, 2H; Rh-$CH_2CH_2$O-); $^{13}C\{^1H\}$ NMR (50.33 MHz, [$D_6$]acetone, 298 K): $\delta = 165.4$ ($Py_b$-C2), 162.6 ($Py_a$-C2), 151.9 ($Py_b$-C6), 150.9 ($Py_a$-C6), 139.4 ($Py_b$-C4), 138.4($Py_a$-C4), 125.9 ($Py_b$-C3), 125.1 ($Py_a$-C3), 124.6 ($Py_b$-C5), 122.2 ($Py_a$-C5), 78.8 (d, $^2J(Rh,C) = 4.0$ Hz; Rh-$CH_2CH_2$O-), 66.8 (N-$CH_2$-$Py_b$), 64.7 (N-$CH_2$-$Py_a$), 1.3 (d, $^1J(C,Rh) = 18.4$ Hz; Rh-$CH_2CH_2$O-); FAB-MS (*m*-Noba/$CH_3CN$): *m*/*z*: 437 $[M^+]$, 393 $[M - CH_2CH_2O]^+$. [**3a**]$^+$ appears to co-precipitate with $H_2O$: anal. calcd for [**3a**]$PF_6 \cdot 1.5\,H_2O$ ($C_{20}H_{25}N_4O_{2.5}RhPF_6$): C 39.42, H 4.14, N 9.20; found: C 38.60, H 3.62, N 9.41; anal. calcd for [**3a**]$(BPh_4) \cdot 1.5\,H_2O$ ($C_{44}H_{45}N_4O_{2.5}RhB$): C 67.44, H 5.79, N 7.15; found: C 67.15, H 5.43, N 7.04.

**($\kappa^2$-*O,C*-2-Oxyethyl)-($\kappa^4$-*N*-[(6-methyl-2-pyridyl)methyl]-*N,N*-di(2-pyridylmethyl)amine)-rhodium(III) tetraphenylborate ([3b]$BPh_4$)**: $[\{(C_2H_4)_2Rh(\mu\text{-}Cl)\}_2]$ (200 mg, 0.51 mmol) and MeTPA (320 mg, 1.05 mmol) were added to MeOH (25 mL) at $-78\,^\circ C$ and the mixture was stirred for 1 h. An aqueous solution of $H_2O_2$ (0.2 mL, 35 %) was added and the solution was allowed to slowly warm to room temperature. Any undissolved material was removed by filtration. $NaBPh_4$ (360 mg, 1.06 mmol) in MeOH (7 mL) was added to the solution. The light yellow solid which precipitated was collected by filtration. After recrystallisation from dichloromethane/hexane, pure [**3b**]$BPh_4 \cdot 1.5\,H_2O$ was obtained as bright yellow crystals which were suitable for X-ray diffraction. Yield: 64 % (654 mg); $^1H$ NMR (200.13 MHz, $CD_2Cl_2$, 298 K): $\delta = 8.77$ (d, $^3J(H,H) = 5.6$ Hz, 2H; $Py_a$-H6), 7.80–6.50 (m, 9H; Py-H4, Py-H5 and Py-H3), 7.36 (m, 8H; BAr-H2, 7.01 (t,$^3J(H,H) = 7.4$ Hz, 8H; BAr-H3), 6.86 (t, $^3J(H,H) = 7.4$ Hz, 4H; BAr-H4), 4.81 (d[AB], $^2J(H,H) = 15.3$ Hz, 2H; N-$CH_2$-$Py_b$), 4.80 (t, $^3J(H,H) = 7.6$ Hz, 2H; Rh-$CH_2CH_2$O-), 4.29 (d[AB], $^2J(H,H) = 15.3$ Hz, 2H; N-$CH_2$-$Py_b$), 4.10 (s, 2H; N-$CH_2$-$Py_a$), 2.83 (s, 3H; $Py_a$-$CH_3$), 2.35 (dt,$^3J(H,H) = 7.6$ Hz, $^2J(H,Rh) = 2.6$ Hz, 2H, Rh-$CH_2CH_2$O-), 2.05 (s, ≈3H; $H_2O$); $^{13}C\{^1H\}$ NMR (75.47 MHz, $CD_2Cl_2$, 298 K): $\delta = 164.7$ (q, $^1J(C,B) = 48.6$ Hz; BAr-C1), 164.5 ($Py_b$-C2), 164.2 ($Py_a$-C2), 161.6 ($Py_a$-C6), 152.5 ($Py_b$-C6), 139.5 ($Py_b$-C4), 138.5($Py_a$-C4), 136.8 (BAr-C2), 125.8 (q, $^3J(C,B) = 2.8$ Hz; BAr-C3), 126.2 ($Py_b$-C3), 125.8 ($Py_a$-C3), 124.6 ($Py_b$-C5), 122.8 (BAr-C4), 119.6 ($Py_a$-C5), 80.6 (d, $^2J(Rh,C) = 4.2$ Hz; Rh-$CH_2CH_2$O-), 66.6 (N-$CH_2$-$Py_b$), 65.5 (N-$CH_2$-$Py_a$), 26.7 ($Py_a$-$CH_3$), 2.5 (d, $^1J(C,Rh) = 18.0$ Hz; Rh-$CH_2CH_2$O-); FAB-MS (*m*-Noba/$CH_2Cl_2$): *m*/*z*: 451 $[M^+]$, 407 $[(M - CH_2CH_2O)^+]$; anal. calcd for [**3b**]$BPh_4 \cdot 1.5\,H_2O$ ($C_{45}H_{47}N_4BO_{2.5}Rh$): C 67.76, H 5.94, N 7.02; found: C 66.96, H 5.81, N 6.94.

**($\kappa^1$-*C*-2-Hydroxyethyl)-(chloro)-($\kappa^4$-*N,N,N*-tri(2-pyridylmethyl)amine)-rhodium(III) tetraphenylborate ([6a]$BPh_4$)**: [**3a**]$BPh_4$ (100 mg, 0.13 mmol) was dissolved in acetone (15 mL) and $NH_4Cl$ (100 mg, 1.89 mmol) was added. The solution was placed in an ultrasonic bath for 15 min, and then was stirred for 45 min at room temperature. The solvent was partially evaporated under vacuum to a volume of ≈3 mL. The solution was carefully top-layered with MeOH (≈10 mL) resulting in the slow crystallisation of [**6a**]$BPh_4 \cdot$MeOH as bright yellow crystals. Yield: 87 % (95 mg); $^1H$ NMR (300.13 MHz, [$D_6$]DMSO, 298 K): $\delta = 8.80$ (d, 1H, $^3J(H,H) = 5.9$ Hz, $Py_a$-H6), 8.56 (d, 2H, $^3J(H,H) = 5.6$ Hz, $Py_b$-H6), 8.0–7.1 (m, 9H, Py-H4, Py-H5 and Py-H3), 7.20 (m, 8H, BAr-H2), 6.93 (t, 8H, $^3J(H,H) = 7.3$ Hz, BAr-H3), 6.82 (t, 4H, $^3J(H,H) = 7.3$ Hz, BAr-H4), 5.51 (d[AB], 2H, $^3J(H,H) = 15.5$ Hz, N-$CH_2$-$Py_b$), 5.04 (s, 2H, N-$CH_2$-$Py_a$), 5.02 (d[AB], 2H, $^3J(H,H) = 15.5$ Hz, N-$CH_2$-$Py_b$), 4.41 (t, 1H, $^3J(H,H) = 5.4$ Hz, Rh-$CH_2CH_2OH$), 4.13 (q, 1H, 4.4 Hz, $CH_3OH$), 3.96 (dt, 2H, $^3J(H,H) = 8.2$ Hz, $^3J(H,H) = 5.4$ Hz, Rh-$CH_2CH_2$OH), 3.18 (d, 3H, $^3J(H,H) = 4.4$ Hz, $CH_3$OH), 3.13 (dt, 2H, $^3J(H,H) = 8.2$ Hz, $^2J(H,Rh) = 2.6$ Hz, Rh-$CH_2CH_2$OH); $^{13}C\{^1H\}$ NMR (75.47 MHz, [$D_6$]DMSO, 298 K): $\delta = 165.0$ ($Py_b$-C2), 164.2 ($Py_a$-C2), 163.4 (q, $^1J(C,B) = 48.5$ Hz; BAr-C1), 150.6 ($Py_b$-C6), 149.2 ($Py_a$-C6), 139.2 ($Py_b$-C4), 138.8($Py_a$-C4), 135.5 (BAr-C2), 125.3 (q, $^3J(C,B) = 2.8$ Hz; BAr-C3), 125.1 ($Py_a$-C3), 124.3 ($Py_b$-C3), 122.1 ($Py_a$-C5), 121.5 (BAr-C4, $Py_b$-C5), 65.9 (N-$CH_2$-$Py_b$), 65.0 (N-$CH_2$-$Py_a$), 64.6 (Rh-$CH_2CH_2$OH), 34.4 (d, $^1J(C,Rh) = 25.0$ Hz, Rh-$CH_2CH_2$OH); FAB-MS (*m*-Noba/$CH_3CN$): *m*/*z*: 473 $[M - BPh_4]^+$, 428 $[M - CH_2CH_2O - BPh_4]^+$, 393 $[M\text{-}CH_2CH_2O - BPh_4 - Cl]^+$; anal. calcd for [**6a**]$BPh_4 \cdot CH_3OH$ ($C_{44}H_{43}N_4OBRhCl$): C 65.51, H 5.74, N 6.79; found: C 65.50, H 6.12, N 6.45.

**($\kappa^1$-*C*-2-Methoxyethyl)-(iodo)-($\kappa^4$-*N,N,N*-tri(2-pyridylmethyl)amine)-rhodium(III) tetraphenylborate ([7a]$BPh_4$)**: [**3a**]$BPh_4$ (60 mg, 0.08 mmol) was dissolved in $CH_2Cl_2$ (10 mL), the solution was cooled to $-80\,^\circ C$ and MeI (2 mL, cooled to $-80\,^\circ C$) was added. The resulting pale yellow solution was allowed to warm to room temperature and was then stirred for 1 h, during which time the colour of the solution gradually changed to bright orange. The solvent was completely evaporated. Slow, partial evaporation of a saturated $CH_3CN$ solution of the crude product gave bright orange crystals of [**7a**]$BPh_4$. Yield: 77 % (55 mg); $^1H$ NMR (300.13 MHz, $CD_2Cl_2$, 298 K): $\delta = 8.94$ (d, 1H, $^3J(H,H) = 5.9$ Hz, $Py_a$-H6), 8.31 (d, 2H, $^3J(H,H) = 6.2$ Hz, $Py_b$-H6), 7.70–6.60 (m, 9H, Py-H4, Py-H5 and Py-H3), 7.41 (m, 8H, BAr-H2), 7.01 (t, 8H, $^3J(H,H) = 7.3$ Hz, BAr-H3), 6.87 (t, 4H, $^3J(H,H) = 7.3$ Hz, BAr-H4), 5.59 (d[AB], 2H, $^3J(H,H) = 15.5$ Hz, N-$CH_2$-$Py_b$), 4.34 (d[AB], 2H, $^3J(H,H) = 15.5$ Hz, N-$CH_2$-$Py_b$), 4.08 (t, 2H, $^3J(H,H) = 6.3$ Hz, Rh-$CH_2CH_2$O-), 4.02 (s, 2H, N-$CH_2$-$Py_a$), 3.55 (s, 3H, -O$CH_3$), 3.28 (dt, 2H, $^3J(H,H) = 6.3$ Hz, $^2J(H,Rh) = 2.9$ Hz, Rh-$CH_2CH_2$O-); $^{13}C\{^1H\}$ NMR (75.47 MHz, $CD_2Cl_2$, 298 K): $\delta = 165.1$ ($Py_b$-C2), 163.7 (q, $^1J(C,B) = 48.5$ Hz; BAr-C1), 163.3 ($Py_a$-C2), 152.2 ($Py_b$-C6), 149.9 ($Py_a$-C6), 139.7 ($Py_b$-C4), 139.4 ($Py_a$-C4), 136.8 (BAr-C2), 126.6 (q, $^3J(C,B) = 2.8$ Hz; BAr-C3), 126.1 ($Py_b$-C3), 125.8 ($Py_a$-C3), 124.6 ($Py_b$-C5), 122.9 (BAr-C4, $Py_a$-C5), 79.8 (Rh-$CH_2CH_2$O-), 68.1 (N-$CH_2$-$Py_b$), 64.4 (N-$CH_2$-$Py_a$), 58.7 (-$OCH_3$), 26.3 (d, $^1J(C,Rh) = 25.0$ Hz, Rh-$CH_2CH_2$O-); FAB-MS (*m*-Noba/$CH_3CN$): *m*/*z*: 579 $[M - BPh_4]^+$, 521 $[M - CH_2CH_2OMe - BPh_4{+}H]^+$, 393 $[M - CH_2CH_2OMe - BPh_4 - I]^+$; anal. calcd for [**7a**]$BPh_4$ ($C_{45}H_{45}N_4OIBRh$): C 60.16, H 5.05, N 6.24; found: C 60.39, H 5.19, N 6.55.

**($\kappa^2$-*N,C*-2-(Acetimidoyloxy)ethyl)-(*N,N,N*-tri(2-pyridylmethyl)amine)rhodium(III) bis(tetraphenylborate) ([8]$(BPh_4)_2$)**: [**3a**]$BPh_4$ (100 mg, 0.13 mmol) was dissolved in $CH_3CN$ (10 mL) and $NH_4PF_6$ (25 mg ,0.15 mmol) was added. The solution was stirred at room temperature for 4 h. Subsequently, $NaBPh_4$ (45 mg, 0.13 mmol) dissolved in $CH_3CN$ (5 mL) was added. The solvent was partially evaporated under vacuum to a volume of ≈5 mL. Addition of MeOH (≈10 mL) precipitated [**8**]$(BPh_4)_2$ as a white powder. Yield: 88 % (131 mg); $^1H$ NMR (200.13 MHz, $CD_3CN$, 298 K): $\delta = 8.70$ (d, 1H, $^3J(H,H) = 5.6$ Hz, $Py_a$-H6), 8.32 (d, 2H, $^3J(H,H) = 5.9$ Hz, $Py_b$-H6), 8.0–6.8 (m, 9H, Py-H4, Py-H5 and Py-H3), 7.31 (m, 8H, BAr-H2), 7.03 (t, 8H, $^3J(H,H) = 7.3$ Hz, BAr-H3), 6.87 (t, 4H, $^3J(H,H) = 7.3$ Hz, BAr-H4), 5.48 (d[AB], 2H, $^3J(H,H) = 16.8$ Hz, N-$CH_2$-$Py_b$), 5.08 (d[AB], 2H, $^3J(H,H) = 16.8$ Hz, N-$CH_2$-$Py_b$), 4.84 (s, 2H, N-$CH_2$-$Py_a$), 4.26 (t, 2H, $^3J(H,H) = 5.6$ Hz, Rh-$CH_2CH_2$O-), 3.38 (dt, 2H, $^3J(H,H) = 5.6$ Hz, $^2J(H,Rh) = 2.7$ Hz, Rh-$CH_2CH_2$O-), 2.11 (s, 3H, -O-C($CH_3$)=N). The $^1H$ NMR spectrum in [$D_6$]DMSO shows an additional signal at $\delta = 8.35$ (br s, 1H, -O-C($CH_3$)=N*H*-); $^{13}C\{^1H\}$ NMR (50.33 MHz, [$D_6$]DMSO, 298 K): $\delta = 179.5$ (-O-*C*($CH_3$)=N), 164.3 ($Py_b$-C2), 163.2 ($Py_a$-C2), 163.4 (q, $^1J(C,B) = 48.6$ Hz; BAr-C1), 150.2 ($Py_b$-C6), 148.8 ($Py_a$-C6), 140.1 ($Py_b$-C4), 139.5 ($Py_a$-C4), 135.6 (BAr-C2), 126.0 ($Py_b$-C3), 125.3 (q, $^3J(C,B) = 2.8$ Hz; BAr-C3, $Py_a$-C3), 124.9 ($Py_b$-C5), 122.3 ($Py_a$-C5), 121.6 (BAr-C4) 71.8 (Rh-$CH_2CH_2$O-), 65.6 (N-$CH_2$-$Py_a$), 64.9 (N-$CH_2$-$Py_b$), 28.4 (d, $^1J(C,Rh) = 26.4$ Hz, Rh-$CH_2CH_2$O-), 21.6 (-O-C($CH_3$)=N); FT-IR (KBr): $\tilde{\nu} = 3605$ (m), 3509 (m), 3275 (m), 1634 (s, C=N) $cm^{-1}$; FAB-MS (*m*-Noba/



0947-6539/00/0601-0310 $ 17.50+.50/0 *Chem. Eur. J.* **2000**, *6*, No. 1

$CH_3CN$): *m*/*z*: 798 $[M-BPh_4]^+$, 478 $[M-H-(BPh_4)_2]^+$, 393 $[M-(CH_2CH_2O\text{-}C(CH_3)\!=\!NH\text{-})-(BPh_4)_2+H]^+$; FAB-MS (*m*-Noba/$CH_3CN$) from a sample prepared from a $CD_3CN$ solution: *m*/*z*: 801 $[M-BPh_4]^+$, 481 $[M-H-(BPh_4)_2]^+$, 393 $[M-(CH_2CH_2O\text{-}C(CD_3)\!=\!NH\text{-})-(BPh_4)_2+H]^+$; anal. calcd for **[8]**$(BPh_4)_2\cdot CH_3OH$ ($C_{71}H_{70}N_5O_2B_2Rh$): C 74.16, H 6.14, N 6.09; found: C 73.50, H 6.32, N 6.02.

**($\kappa^2$-*O*,*C*-2-(Acetylamino)ethyl)-(*N*,*N*,*N*-tri(2-pyridylmethyl)amine)-rhodium(III) bis(tetraphenylborate) ([9](BPh$_4$)$_2$)**: **[3a]**$BPh_4$ (100 mg, 0.13 mmol) was dissolved in $CH_3CN$ (10 mL) and $NH_4PF_6$ (45 mg, 0.28 mmol) was added. The solution was heated to 65 °C for 4 h. $NaBPh_4$ (90 mg, 0.26 mmol) dissolved in $CH_3CN$ (5 mL) was added. The solvent was partially evaporated under vacuum to a volume of ≈3 mL. The solution was left to stand which resulted in the slow crystallisation of **[9]**$(BPh_4)_2\cdot CH_3CN$ as transparent/white crystals which were suitable for X-ray diffraction. Yield: 71% (107 mg); $^1$H NMR (200.13 MHz, $CD_3CN$, 298 K): $\delta = 8.59$ (d, 1H, $^3J(H,H) = 6.2$ Hz, $Py_a$-H6), 8.43 (d, 2H, $^3J(H,H) = 5.9$ Hz, $Py_b$-H6), 8.0–6.8 (m, 9H, Py-H4, Py-H5 and Py-H3), 7.31 (m, 8H, BAr-H2), 7.03 (t, 8H, $^3J(H,H) = 7.3$ Hz, BAr-H3), 6.87 (t, 4H, $^3J(H,H) = 7.3$ Hz, BAr-H4), 5.45 (d[AB], 2H, $^3J(H,H) = 15.9$ Hz, N-$CH_2$-$Py_b$), 5.07 (d[AB], 2H, $^3J(H,H) = 15.9$ Hz, N-$CH_2$-$Py_b$), 4.94 (s, 2H, N-$CH_2$-$Py_a$), 3.47 (dt, 2H, $^3J(H,H) = 5.9$ Hz, $^3J(Rh,H) = 2.4$ Hz, Rh-$CH_2CH_2$NH-), 3.23 (t, 2H, $^3J(H,H) = 5.9$ Hz, Rh-$CH_2CH_2$NH-), 1.80 (s, 3H, NH-C($CH_3$)=O-). The $^1$H NMR spectrum in [D$_6$]DMSO shows an additional signal at $\delta = 9.81$ (br s, 1H, *NH*-); $^{13}$C{$^1$H} NMR (50.33 MHz, [D$_6$]DMSO, 298 K): $\delta = 178.8$ (NH-*C*($CH_3$)=O-), 164.9 ($Py_b$-C2), 164.3 ($Py_a$-C2), 163.4 (q, $^1J(C,B) = 48.6$ Hz; BAr-C1), 150.7 ($Py_a$-C6), 150.4 ($Py_b$-C6), 140.3 ($Py_b$-C4), 139.4 ($Py_a$-C4), 135.6 (BAr-C2), 125.9 ($Py_b$-C3), 125.3 (q, $^3J(C,B) = 2.8$ Hz; BAr-C3, $Py_a$-C3), 124.8 ($Py_b$-C5), 122.5 ($Py_a$-C5), 121.6 (BAr-C4) 118.1 (free $CH_3CN$), 65.4 (N-$CH_2$-$Py_b$), 63.9 (N-$CH_2$-$Py_a$), 41.5 (Rh-$CH_2CH_2$NH-), 33.3 (d, $^1J(C,Rh) = 27.7$ Hz, Rh-$CH_2CH_2$NH-), 21.5 (NH-C($CH_3$)=O-), 1.2 (free $CH_3CN$); FT-IR (KBr): $\tilde{\nu} = 3307$ (s, NH), 1600 cm$^{-1}$ (s, C=N); FAB-MS (*m*-Noba/$CH_3CN$): *m*/*z*: 798 $[M-BPh_4]^+$, 478 $[M-H-(BPh_4)_2]^+$, 393 $[M-(CH_2CH_2NH\text{-}C(CH_3)\!=\!O\text{-})-(BPh_4)_2+H]^+$; anal. calcd for **[9]**$(BPh_4)_2\cdot CH_3CN$ ($C_{72}H_{69}N_6ORhB_2$): C 74.62, H 6.00, N 7.25; found: C 74.68, H 6.50, N 7.21.

**($\kappa^2$-*O*,*C*-2-(1-Methoxy-1-methylethoxy)ethyl)-(*N*,*N*,*N*-tri(2-pyridylmethyl)-amine)rhodium(III) tetraphenylborate ([10]BPh$_4$)**: **[3a]**$BPh_4$ (100 mg, 0.13 mmol) was dissolved in acetone (10 mL). The solution was stirred at room temperature for seven days. The product was precipitated as a white powder by the addition of $Et_2O$ (≈50 mL). $^1$H NMR (200.13 MHz, [D$_6$]acetone, 298 K): $\delta = 8.74$ (d, 2H, $^3J(H,H) = 5.6$ Hz, $Py_b$-H6), 8.67 (d, 1H, $^3J(H,H) = 5.6$ Hz, $Py_a$-H6), 8.0–6.8 (m, 9H, Py-H4, Py-H5 and Py-H3), 7.36 (m, 8H, BAr-H2), 6.93 (t, 8H, $^3J(H,H) = 7.1$ Hz, BAr-H3), 6.78 (t, 4H, $^3J(H,H) = 7.1$ Hz, BAr-H4), 5.55 (d[AB], 2H, $^3J(H,H) = 14.7$ Hz, N-$CH_2$-$Py_b$), 5.09 (s, 2H, N-$CH_2$-$Py_a$), 4.98 (d[AB], 2H, $^3J(H,H) = 14.7$ Hz, N-$CH_2$-$Py_b$), 3.55 (t, 2H, $^3J(H,H) = 5.6$ Hz, Rh-$CH_2CH_2$O-), 3.14 (dt, 2H, $^3J(H,H) = 5.6$ Hz, $^2J(H,Rh) = 2.7$ Hz, Rh-$CH_2CH_2$O-), 0.60 (s, 6H, -O-C($CH_3$)$_2$-O); FAB-MS (*m*-Noba/$CH_3CN$): *m*/*z*: 453, 428, 391; FAB-MS (*m*-Noba/$CH_3CN$) from a sample prepared from an [D$_6$]acetone solution: *m*/*z*: 589, 452, 438, 429, 394, 391.

## Acknowledgements

We thank Johnson Matthey Ltd. for a generous loan of $RhCl_3\cdot 3H_2O$.


[1] a) T. Linker, *Angew. Chem.* **1997**, 109, 2150; *Angew. Chem. Int. Ed. Engl.* **1997**, *36*, 2060; b) N. S. Finney, P. J. Pospisil, S. Chang, M. Palucki, R. G. Konsler, K. B. Hansen, E. N. Jacobsen, *Angew. Chem.* **1997**, *109*, 1798; *Angew. Chem. Int. Ed. Engl*, **1997**, *36*, 1720; c) C. Linde, M. Arnold, P.-O. Norrby, B. Åkermark, *Angew. Chem.* **1997**, *109*, 1802; *Angew. Chem. Int. Ed. Engl*, **1997**, *36*, 1723.

[2] Excellent overviews are given in: a) K. A. Jørgensen, *Chem. Rev.* **1989**, *89*, 431; b) K. A. Jørgensen, B. Schiøtt, *Chem. Rev.* **1990**, *90*, 1483.

[3] See, for example: a) F. Freeman, C. O. Fuselier, C. R. Armstead, C. E. Dalton, P. A. Davidson, E. M. Karchesfski, D. E. Krochman, M. N. Johnson, N. K. Jones, *J. Am. Chem. Soc.* **1981**, *103*, 1154; b) D. G. Lee, N. A. Noureldin, *J. Am. Chem. Soc.* **1983**, *105*, 3188; c) A. K. Rappé, W. A. Goddard, *J. Am. Chem. Soc.* **1982**, *104*, 3287; d) M. Schröder, E. C. Constable, *J. Chem. Soc. Chem. Commun.* **1982**, 734.

[4] J. Blum, B. Zinger, D. Milstein, O. Buchman, *J. Org. Chem.* **1978**, *43*, 2961.

[5] J. Bakos, Á. Orosz, S. Cscrépi, I. Tóth, D. Sinou, *J. Mol. Catal. A: Chem.* **1997**, *116*, 85.

[6] 2-Metallaoxetanes stabilised by exocyclic double bonds have been synthesised by the reaction of a peroxo-metal complex with a ketene: a) S. Baba, T. Ogura, S. Kawaguchi, H. Tokunan, Y. Kai, N. Kashi, *J. Chem. Soc. Chem. Commun*, **1972**, 910; b) L. Pandolfo, G. Paiaro, G. Valle, P. Ganis, *Gazz Chim. Ital.* **1985**, *115*, 65; c) W. A. Herrmann, U. Küsthardt, A. Schäfer, E. Herdtweck, *Angew. Chem.* **1986**, *98*, 818; *Angew. Chem. Int. Ed. Engl.* **1986**, *25*, 817.

[7] a) R. Schlodder, J. A. Ibers, M. Lenarda, M. Graziani, *J. Am. Chem. Soc*. **1974**, *96*, 6893; b) M. Lenarda, N. B. Pahor, M. Calligaris, M. Graziani, L. Randaccio, *J. Chem. Soc. Dalton Trans.* **1978**, 279; c) D. P. Klein, J. C. Hayes, R. G. Bergman, *J. Am. Chem. Soc.* **1988**, *110*, 3704; d) V. W. Day, W. G. Klemperer, S. P. Lockledge, D. J. Main, *J. Am. Chem. Soc*. **1990**, *112*, 2031; e) J. C. Hartwig, R. G. Bergman, R. A. Andersen, *Organometallics* **1991**, *10*, 3344; f) J. C. Hartwig, R. G. Bergman, R. A. Andersen, *J. Am. Chem. Soc.* **1990**, *112*, 3234.

[8] a) A. A. Zlota, F. Frolow, D. Milstein, *J. Am. Chem. Soc.* **1990**, *112*, 6411; b) M. J. Calhorda, A. M. Galvão, C. Ünaleroglu, A. A. Zlota, F. Frolow, D. Milstein, *Organometallics* **1993**, *12*, 3316.

[9] a) B. de Bruin, M. J. Boerakker, J. J. J. M. Donners, B. E. C. Christiaans, P. P. J. Schlebos, R. de Gelder, J. J. M. Smits, A. L. Spek, A. W. Gal, *Angew. Chem. Int. Ed. Engl.* **1997**, *36*, 2064; *Angew. Chem.* **1997**, 109, 2153; b) B. de Bruin, M. J. Boerakker, R. de Gelder, J. M. M. Smits, A. W. Gal, *Angew. Chem*. **1999**, *111*, 118–121; *Angew. Chem. Int. Ed.* **1999**, *38*, 219–222.

[10] H. Yang, N. Lugan, R. Matieu, *Organometallics* **1997**, *16*, 2089.

[11] Y. Hayashi, T. Kayatani, H. Sugimoto, M. Suzuki, K. Inomata, A. Uehara, Y. Mizutani, T. Kitagawa, Y. Maeda, *J. Am. Chem. Soc.* **1995**, *117*, 11220.

[12] Results with $Cu^{II}$ complexes, however, show that substitution of a pyridyl by a 6-methylpyridyl donor does not always lead to longer a M–N bond length: H. Nagao, N. Komeda, M. Mukaida, M. Suzuki, K. Tanaka, *Inorg. Chem*. **1996**, *35*, 6809.

[13] A. R. Rossi, R. Hoffmann, *Inorg. Chem.* **1975**, *14* (2), 365.

[14] a) M. Brookhart, D. M. Lincoln, M. A. Bennet, S. Pelling, *J. Am. Chem. Soc*. **1990**, *112*, 2691; b) L. Öhrström, S. Strömberg, J. Glaser, K. Zetterberg, *J. Organomet. Chem*. **1998**, *558*, 123; c) M. A. Ciriano, M. J. Fernández, J. Modegro, M. J. Rodríguez, L. A. Oro, *J. Organomet. Chem.* **1993**, *443*, 249 and references therein.

[15] a) C. K. Ghosh, W. A. G. Graham, *J. Am. Chem. Soc.* **1989**, *111*, 375; b) N. B. Pahor, R. Dreos-Garlatti, S. Geremia, L. Randaccio, G. Tauzer, E. Zangrando, *Inorg. Chem.* **1990**, *29*, 3437; c) A. C. Skapski, P. G. H. Troughton, *J. Chem. Soc. Chem. Commun.* **1969**, 666.

[16] a) M. Green, D. M. Grove, J. L. Spencer, F. G. A. Stone, *J. Chem. Soc. Dalton Trans.* **1977**, 2228; b) J. Evans, B. F. G. Johnson, J. Lewis, *J. Chem. Soc. Chem. Commun*. **1971**, 1252; c) R. A. Henderson, K. E. Oglieve, *J. Chem. Soc. Chem. Commun.* **1991**, 584.

[17] a) R. G. Ball, C. K. Ghosh, J. K. Hoyano, A. D. McMaster, W. A. G. Graham, *J. Chem. Soc. Chem. Commun*. **1989**, 341; b) H. Werner, H. J. Scholz, R. Zolk, *Chem. Ber.* **1985**, *118*, 4531; c) D. Wang, R. J. Angelici, *Inorg. Chem.* **1996**, *35*, 1321; d) M. Brookhart, D. M. Lincoln, *J. Am. Chem. Soc*. **1988**, *110*, 8719; e) H. Werner, R. Feser, *Angew. Chem*. **1979**, *91*, 171; *Angew. Chem. Int. Ed. Engl.* **1979**, *18*, 157, and references therein.

[18] a) S. E. Kegley, C. J. Schaverien, J. H. Freudenberger, R. G. Bergman, S. P. Nolan, C. D. Hoff, *J. Am. Chem. Soc*. **1987**, *109*, 6563; b) Y. J. Kim, K. Osakada, A. Takenaka, A, Yamamoto, *J. Am. Chem. Soc.* **1990**, *112*, 1096; c) G. M. Kapteijn, A. Dervisi, D. M. Grove, H. Kooijman, M. T. Lakin, A. L. Spek, G. van Koten, *J. Am. Chem. Soc* **1995**, *117*, 10939; d) C. D. Bugno, M. Pasquali, P. Leoni, P. Sabatino, D. Braga, *Inorg. Chem.* **1989**, *28*, 1390.

[19] a) M. P. Doyle, W. R. Winchester, S. H. Simonsen, R. Ghosh, *Inorg. Chim. Acta* **1994**, *220*, 193; b) P. Caddy, M. Green, J. A. K. Howard, J. M. Squire, N. J. White, *J. Chem. Soc. Dalton Trans.* **1981**, 400; c) M. A. Calvo, A. M. M. Lanfredi, L. A. Oro, M. R. Pinillos, C. Tejel, A. Tiripicchio, F. Ugozzoli, *Inorg. Chem.* **1993**, *32*, 1147.

[20] Oxidation of tertiary amines by $H_2O_2$ has been proposed to involve an attack by the $OH^+$ moiety of $H_2O_2$: J. March, *Advanced Organic Chemistry*, 4th ed., Wiley, **1992**, p. 1200.
[21] P. T. Matsunaga, G. L. Hillhouse, *J. Am Chem. Soc*. **1993**, *115*, 2075.
[22] M. Brookhart, B. Grant, A. F. Volpe, Jr, *Organometallics*, **1992**, *11*, 3920.
[23] D. Milstein, *J. Am. Chem. Soc*. **1982**, *104*, 5227.
[24] D. Milstein, J. C. Calabrese, *J. Am. Chem. Soc*. **1982**, *104*, 3773.
[25] M. D. Fryzuk, P. A. MacNeil, S. J. Rettig, *J. Am. Chem. Soc*. **1987**, *109*, 2803.
[26] For the intramolecular Pinner reaction from $[(PMe_3)_4Ir^{III}(CH_2OH)(N{\equiv}CMe)]^{2+}$ to $\kappa^2$-*N,C*-2-(acetimidoyloxy)-methyl complex $[(PMe_3)_4Ir^{III}$-$(CH_2O$-$C(Me){=}NH)]^{2+}$, see: D. L. Thorn, J. C. Calabrese, *J. Organomet. Chem*. **1984**, *272*, 283. For other examples of nitrile C≡N-bond activation by metal-coordination (including Pinner-type reactions with alcohols), see: B. N. Storhoff, H. C. Lewis, Jr, *Coord. Chem. Rev*. **1977**, *23*, 1.
[27] J. March, *Advanced Organic Chemistry*, 4th ed, John Wiley & Sons, **1992**. For the Pinner syntheses see p. 892, and references therein. For the Ritter reaction see p. 970, and references therein.
[28] a) P. Schnider, G. Koch, P. Pretot, G. Wang, F. M. Bohnen, C. Kruger, A. Pfaltz, *Chem. Eur. J.* **1997**, *2*, 887; b) H. Nishiyama, M. Kondo, T. Nakamura, K Itoh, *Organometallics* **1991**, *10*, 500; c) M. Ghedini, M. Longeri, F. Neve, A. M. M. Lanfredi, A. Tripicchio, *J. Chem. Soc. Dalton Trans.* **1989**, 1217. See also ref. [26].
[29] a) O. Heilmann, H. D. Hausen, W. Kaim, *Z. Naturforsch*, *Teil B* **1994**, *49*, 1554; b) B. McCullogh, J. Halpern, M. R. Thompson, C. R. Landis, *Organometallics* **1990**, *9*, 1392; c) M. Costa, G. P. Chiusoli, F. Salvadori, G. Bocelli, *Gazz. Chim. Ital.* **1995**, *125*, 589; d) B. E. Villarroya, L. A. Oro, F. J. Lahoz, A. J. Edwards, M. A. Ciriano, P. A. Alonso, A. Tiripicchio, M. Tiripicchio Camellini, *Inorg. Chim. Acta* **1996**, *250*, 241; e) M. I. Arriortua, J. L. Pizarro, J. Ruiz, J. M. Morena, E. Colacio, *Inorg. Chim. Acta* **1995**, *231*, 103; f) G. Bocelli, G. P. Chiusoli, M. Costa, M. Michelotti, *J. Chem. Soc. Perkin Trans. 1* **1994**, 1347; g) N. W. Alcock, J. M. Brown, P. J. Maddox, *J. Chem. Soc. Chem. Comm.* **1986**, 1532; g) N. W. Alcock, J. M. Brown, A. E. Derome, A. R. Lucy, *J. Chem. Soc. Chem. Comm.* **1985**, 575.
[30] Thermal decomposition of alkyl-alkanimidates yields, among others, nitriles and alcohols or trisubstituted 1,3,5-triazines and alcohols: a) F. Cramer, K. Pawelzik, J. Kupper, *Angew. Chem.* **1956**, *20*, 649; b) P. Reynaud, R. C. Moreau, *Bull. Soc. Chim. Fr.* **1964**, 2997. See also references quoted in ref. [31].
[31] F. Cramer, N. Hennrich, *Chem. Ber*. **1961**, 976, and references therein.
[32] a) D. M. Roundhill, *Chem. Rev.* **1992**, *29*, 1; b) D. M. Roundhill, *Catal. Today* **1997**, *37*, 155; c) J. J. Brunet, *Gaz. Chim. Ital.* **1997**, *127*, 111.
[33] a) M. Beller, M. Eichberger, H. Trauthwein, *Angew. Chem*. **1997**, *109*, 2306; *Angew. Chem. Int. Ed. Engl.* **1997**, *36*, 2225; b) J. J. Brunet, G. Commenges, D. Neibecker, K. Philippot, *J Organomet. Chem.* **1994**, *469*, 221; c) A. L. Casalnuovo, J. C. Calabresse, D. Milstein, *J. Am. Chem. Soc*. **1988**, *110*, 6738; d) R. Dorta, P. Egli, F. Zürcher, A. Togni, *J. Am. Chem. Soc.* **1997**, *119*, 10857; e) M. A. Giardello, V. P. Conticello, L. Bard, M. R. Gagné, T. J. Marks, *J. Am. Chem. Soc*. **1994**, *116*, 10241; f) Y. Li, T. J. Marks, *J. Am. Chem. Soc*. **1996**, *118*, 9295; g) Y. Li, T. J. Marks, *Organometallics* **1996**, *15*, 3770; h) A. L. Seligson, W. C. Trogler, *Organometallics* **1993**, *12*, 744, and references therein.
[34] M. J. Calhorda, A. M. Galvão, C. Ünaleroglu, A. A. Zlota, F. Frolow, D. Milstein, *Organometallics* **1993**, *12*, 3316.
[35] J. Blum, B. Zinger, D. Milstein, O. Buchman, *J. Org. Chem.* **1978**, *43*, 2961.
[36] Y. Kamiya, K. Kawato, H. Ohta, *Chem. Lett*. **1980**, 1549.
[37] R. J. de Pasquale, *J. Chem. Soc. Chem. Comm*. **1973**, 157.
[38] a) J. P. Collman, L. S. Hegedus, J. R. Norton, R. G. Finke, *Principles and Applications of Organotransition Metal Chemistry*, University Science, Mill Valley, CA, **1987**; p. 322; b) K. Koo, G. L. Hillhouse, A. L. Rheingold, *Organometallics* **1995**, *14*, 456; c) K. Koo, G. L. Hillhouse, *Organometallics* **1995**, *14*, 4421, and references therein.
[39] a) G. Mann, J. F. Hartwig, *J. Am Chem. Soc*. **1996**, *118*, 13109; b) R. A. Widenhoefer, H. A. Zhong, S. L. Buchwald, *J. Am Chem. Soc.* **1997**, *119*, 6787; c) R. Han, G. L. Hillhouse, *J. Am Chem. Soc.* **1997**, *119*, 8135.
[40] Yields range from 16–27%. Remarkably, acyclic alkyl-alkoxide nickel(II) complexes are reluctant to undergo reductive elimination: a) P. T. Matsunaga, G. L. Hillhouse, *J. Am Chem. Soc*. **1993**, *115*, 2075; b) P. T. Matsunaga, J. C. Mavropoulos, G. L. Hillhouse, *Polyhedron* **1995**, *14*, 175.
[41] a) R. A. Sheldon, J. K. Kochi, *Metal Catalyzed Oxidations of Organic Compounds*, Academic Press, **1981**; b) H. Mimoun in *Comprehensive Coordination Chemistry*, *Vol. 6* (Ed. G. Wilkinson), **1987**, Chapt. 61.3; c) R. S. Dickson, *Homogeneous Catalysis with Compounds of Rhodium and Iridium*, D. Reidel Publishing Company, Dordrecht, **1985**, Chapt. 5; d) E. S. Gore in *Chemistry of the Platinum Group Metals: Recent Developments; Studies in Inorganic chemistry*, *Vol. 11* (Ed.: F. R. Hartley), Elsevier, Amsterdam, Chapt. 8, **1991**; e) J. T. Groves in *Metal Ion Activation of Dioxygen* (Ed.: T. G. Spiro), Wiley, **1980**.
[42] R. Cramer, J. A. McCleverty, J. Bray, *Inorg. Synth.* **1990**, *28*, 86.
[43] G. Anderegg, F. Wenk, *Helv. Chim. Acta* **1967**, *50* (243), 2330.
[44] H. Nagao, N. Komeda, M. Mukaida, M. Suzuki, K. Tanaka, *Inorg. Chem.* **1996**, *35*, 6809.
[45] A. C. T. North, D. C. Philips, F. S. Mathews, *Acta Crystallogr. Sect. A* **1968**, *24*, 351.
[46] P. T. Beurskens, G. Beurskens, W. P. Bosman, R. de Gelder, S. Garcia-Granda, R. O. Gould, R. Israël, J. M. M. Smits; DIRDIF-96. A computer program system for crystal structure determination by Patterson methods and direct methods applied to difference structure factors; Crystallography Laboratory, University of Nijmegen (The Netherlands), **1996**.
[47] P. T. Beurskens, G. Beurskens, M. Strumpel, C. E. Nordman in *Patterson and Pattersons* (Eds: J. P. Glusker, B. K. Patterson, M. Rossi), Clarendon Press, Oxford, **1987**, p. 356.
[48] G. M. Sheldrick, SHELXL-97, Program for the refinement of crystal structures, Universität Göttingen (Germany), **1997**.
[49] A. L. Spek, *Acta Crystallogr. Sect. A* **1990**, 46, C-34.

Received: April 14, 1999 [F1723]

  0947-6539/00/0601-0312 $ 17.50+.50/0 